REPORT DOCUMENTATION PAGE

Form Approved
OMB No. 0704-0188

1a. REPORT SECURITY CLASSIFICATION UNCLASSIFIED	1b. RESTRICTIVE MARKINGS
2a. SECURITY CLASSIFICATION AUTHORITY	3. DISTRIBUTION/AVAILABILITY OF REPORT Approved for public release, distribution unlimited.
2b. DECLASSIFICATION/DOWNGRADING SCHEDULE	
4. PERFORMING ORGANIZATION REPORT NUMBER(S) ATA 87-001	5. MONITORING ORGANIZATION REPORT NUMBER(S)
6a. NAME OF PERFORMING ORGANIZATION Applied Technology Associates 6b. OFFICE SYMBOL (If applicable)	7a. NAME OF MONITORING ORGANIZATION U.S. Army Ballistic Research Laboratory ATTN: SLCBR-LF
6c. ADDRESS (City, State, and ZIP Code) P.O. Box 19434 Orlando, FL 32814	7b. ADDRESS (City, State, and ZIP Code) Aberdeen Proving Ground, MD 21005-5066
8a. NAME OF FUNDING/SPONSORING ORGANIZATION 8b. OFFICE SYMBOL (If applicable)	9. PROCUREMENT INSTRUMENT IDENTIFICATION NUMBER DAAA15-86-C-0069
8c. ADDRESS (City, State, and ZIP Code)	10. SOURCE OF FUNDING NUMBERS PROGRAM ELEMENT NO. / PROJECT NO. / TASK NO. 00 / WORK UNIT ACCESSION NO. 001 AJ

11. TITLE (Include Security Classification)

Base Drag Reduction Using Angled Injection

12. PERSONAL AUTHOR(S)

CAVALLERI, R.J.

13a. TYPE OF REPORT	13b. TIME COVERED	14. DATE OF REPORT (Year, Month, Day)	15. PAGE COUNT
Contract Report	FROM _____ TO _____		

16. SUPPLEMENTARY NOTATION

17. COSATI CODES			18. SUBJECT TERMS (Continue on reverse if necessary and identify by block number)
FIELD	GROUP	SUB-GROUP	

19. ABSTRACT (Continue on reverse if necessary and identify by block number)

Reducing the drag of cannon launched artillery shells is a potential method of increasing the range of the shell. The base drag of the shell is directly related to the base pressure that exists on the base region area. A potential method to reduce the base drag is to employ a solid propellant gas generator located in the shell aft end that injects gas into the base region. The mass injected can be distributed in a number of ways. It can be introduced through the center of the projectile, near the edge of the projectile or a combination of these techniques.

The Phase I SBIR effort concentrated on analyzing the effects of central injection or edge injection and its effect on the base drag. The injectant was injected at subsonic velocities. The injectant was considered to be either air or a mixture of air and hydrogen. The effect of

(Continued on Reverse Side of Form)

20. DISTRIBUTION/AVAILABILITY OF ABSTRACT	21. ABSTRACT SECURITY CLASSIFICATION
☒ UNCLASSIFIED/UNLIMITED ☐ SAME AS RPT. ☐ DTIC USERS	UNCLASSIFIED
22a. NAME OF RESPONSIBLE INDIVIDUAL Walter B. Sturek	22b TELEPHONE (Include Area Code) (301) 278-4773
22c. OFFICE SYMBOL SLCBR-LF-C	

19. ABSTRACT (Continued)

injectant temperature was considered for the air injection case. The air hydrogen mixture was considered to be both non reacting and also reacting. A flame sheet combustion model was employed for the reacting flow case. The free stream Mach numbers considered were 1.4, 1.8, and 2.2. The effect of spin on the base drag was also investigated by including a spin term in the axisymmetric flow equations.

REPORT #ATA-87-001

BASE DRAG REDUCTION USING ANGLED INJECTION

by R.J. CAVALLERI

APPLIED TECHNOLOGY ASSOCIATES
P.O. BOX 149434
ORLANDO FL 32814

8 JUNE 1987

FINAL REPORT

PREPARED FOR

DEPARTMENT OF THE ARMY
BALLISTIC RESEARCH LABORATORIES
ABERDEEN PROVING GROUND
ABERDEEN, MD 21010

CONTRACT; DAAA15-86-C-0069

PROJECT SUMMARY

Reducing the drag of cannon launched artillery shells is a potential method of increasing the range of the shell. The base drag of the shell is directly related to the base pressure that exists on the base region area. A potential method to reduce the base drag is to employ a solid propellant gas generator located in the shell aft end that injects gas into the base region. The mass injected can be distributed in a number of ways. It can be introduced through the center of the projectile, near the edge of the projectile or a combination of these techniques.

The Phase I SBIR effort concentrated on analyzing the effects of central injection or edge injection and its effect on the base drag. The injectant was injected at subsonic velocities. The injectant was considered to be either air or a mixture of air and hydrogen. The effect of injectant temperature was considered for the air injection case. The air hydrogen mixture was considered to be both non reacting and also reacting. A flame sheet combustion model was employed for the reacting flow case. The free stream Mach numbers considered were 1.4, 1.8, and 2.2. The effect of spin on the base drag was also investigated by including a spin term in the axisymmetric flow equations.

The results obtained indicate that subsonic base injection can be beneficial in reducing base drag. The use of edge injection gives higher values of base drag reduction (by approximately 20%) than center injection. Use of higher temperature injectant gas also gives larger values of base drag reduction. It appears that small injection amounts of burning gas in the base region is more beneficial than large amounts, which might blow off the base bubble.

Details of the optimum injection scheme, however, still remain to be determined. In particular, effects of flow channels located in the base region that direct the flow either radially inward or outward may increase or possibly decrease the base pressure and therefore alter the range of the artillery shell.

TABLE OF CONTENTS

LIST OF ILLUSTRATIONS

LIST OF TABLES

ABSTRACT

Reducing the drag of cannon launched artillery shells is a potential method of increasing the range of the shell. The base drag of the shell is directly related to the base pressure that exists on the base region area. A potential method to reduce the base drag is to employ a solid propellant gas generator located in the shell aft end that injects gas into the base region The mass injected can be distributed in a number of ways. It can be introduced through the center of the projectile, near the edge of the projectile or a combination of these techniques.

The Phase I SBIR effort concentrated on analyzing the effects of central injection or edge injection and its effect on the base drag. The injectant was injected at subsonic velocities. The injectant was considered to be either air or a mixture of air and hydrogen. The effect of injectant temperature was considered for the air injection case. The air hydrogen mixture was considered to be both non reacting and also reacting. A flame sheet combustion model was employed for the reacting flow case. The free stream Mach numbers considered were 1.4, 1.8, and 2.2. The effect of spin on the base drag was also investigated by including a spin term in the axisymmetric flow equations.

INTRODUCTION

Reducing the drag of a cannon launched artillery shell is a potential method of increasing the range of the shell. The base drag of the shell is directly related to the base pressure that exists on the base region area. A generic artillery shell is illustrated in Figure 1a. By contouring or boat tailing the back end of the shell as shown in Figure 1b, drag is reduced since the pressure that occurs on the forward facing base region area is not as low as the base pressure and causes a positive axial pressure force. An alternative approach is to employ a solid propellant gas generator that injects gas into the base region as illustrated in Figure 1c. The mass injected can be distributed in a number of ways. It can be introduced through the center of the projectile, near the edge of the projectile or a combination of these techniques.

The effort to be reported on was purely an analytical study and concentrated on central and edge mass injection. The equations employed in the study were the axisymmetric Navier Stokes equations. In addition to the theoretical studies performed some code modifications were required and some relevant software for pre and post processing was developed. Prior to discussing the theoretical results the pre and post processor software will be discussed then the code modifications and finally the results obtained.

GRID GENERATOR PROGRAM

An IBM PC/AT was used to develope the pre and post processor computer programs. The programs were written in Fortran and used the IBM professional Fortran compiler. The IBM AT was also used to communicate with the CRAY X/MP at the Ballistic Research Laboratory using a 1200 baud modem and a terminal emulator software program call PC Plot.

The transformation which generates the physical grid was modified to allow for grid point clustering in the horizontal and vertical direction. Several grid clustering transformations were incorporated into the program. They consisted of an axial grid clustering at one x location and a choice of three vertical clustering techniques. These are

1. a cosine clustering
2. clustering near the centerline
3. clustering at one vertical y position

A pre-processor graphics program for grid visualization was constructed. This program was used to determine if suffucient grid resolution is achieved for the particular case of interest. The original mode of operation for this grid program was to

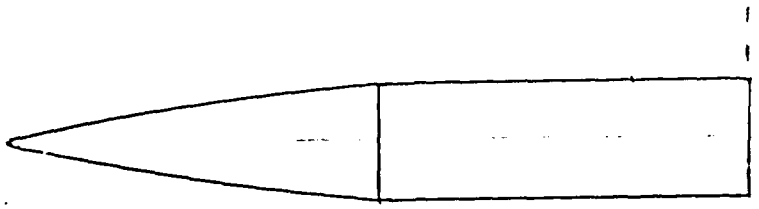

GENERIC SHELL

FIGURE 1a

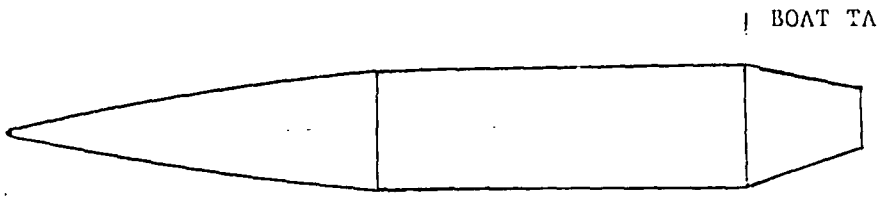

BOAT TAILED SHELL

FIGURE 1b

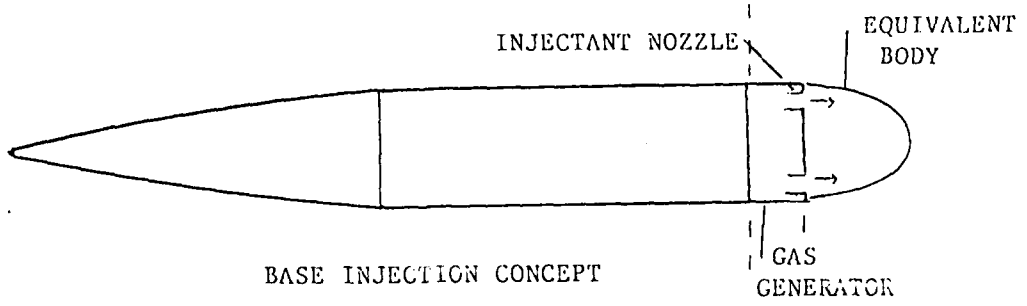

BASE INJECTION CONCEPT

FIGURE 1c

ARTILLERY SHELL CONFIGURATIONS

FIGURE 1

submit the NASJIN code to the main frame as a batch job for an iteration of one time step. The grid generated was then downloaded to the IBM-PC and plotted using the grid program. This method of operation became cumbersome when modifications to the grid such as clustering parameters were used to change the grid resolutuon. This mode of operation was then replaced by using the IBM AT to perform the grid generation. The same grid generator that was in the NASJIN code was implemented on the IBM AT. After selecting the appropiate x and y clustering values, these values were then used in the input to the NASJIN code. This eliminated the submission of a number of one iteration cases with different clustering values and the downloading of the resulting grids. Also this approach minimizes computer charges incurred on the main frame.

Another reason for doing the pre and post processing graphics on the IBM PC is to make the graphics software mainframe independent. Thus when the NASJIN code is ported to another mainframe the graphics will not have to be modified for that mainframe.

GRAPHICS POST PROCESSOR PROGRAM

To display resulting flow field quantities a plotting package was created. This allows visual examination of the resulting flow field predicted by the NASJIN code. The plots that are possible with this program are contour plots, velocity vector plots and flow field profile plots on constant x or y grid lines. The program also has the ability to allow selecting windows to view the flow field. This option permits enlarging sections of the overall flow field to examine details of a particular flowfield region. These changes have not yet been checked out with the plot output from the NASJIN code. The use of this graphics program would allow determining the extent and location of flow characteristics such as separated flow and shock waves. This graphics program uses a software package that runs on the IBM AT called Multi-Halo and is a commercial graphics package.

The method of operation for the graphics program was to submit a case or a number of cases to the CRAY. After these cases ran the plot file generated by thes cases would be downloaded to the IBM AT and the plots generated on the screen. Hard copies of these plots would then be obtained by using a pen plotter. In attempting to do this two problems areas surfaced. The first was the size of the plot file. Although the plot file is not large, to download the file would take on the order of an hour on a 1200 baud line. The other difficulty encountered was the noise on the phone line. During attempting to download a plot file, noise would come across the screen. It is not known if this noise interferred with the data that was transmitted or was only related to the display on the screen. Another possibility is that the PC-PLOT software was inadequate in filtering of the noise.

ADAPTIVE GRID

The incorporation of an adaptive grid capabilty into the NASJIN code (in fact any CFD code) would enhance the codes ability to resolve regions of high gradients. Also it could reduce computer cpu time by allowing use of fewer grid points, since sufficient grid points would be relocated to high gradient regions from low gradient regions. In order to accomplish this a copy of the adaptive grid program was obtained from NASA AMES Research Center (1).

The adaptive grid program obtained utilizes an existing flow field solution to relocate grid points according to local flow gradients. These flow gradients are utilized in a tension/torsion spring analogy to redistribute grid points. Spring tension and torsion coefficients are additional inputs required by the code. An iterative (human in the loop) process is required to determine the correct combination and magnitude of these coefficients to achieve an acceptable solution from the adaptive grid code. The end objective for the adaptive grid code was to have the ability to run the adaptive grid code as a subroutine in the NASJIN code. The original grid and metrics are provided to the NASJIN code, and these metrics are recomputed during the solution process at specified iteration values.

There are two versions of the NASA Ames two dimensional adaptive grid code. The first and older version did not have the ability to perform grid adaption unles it was used in a manual (person in the loop) mode. The second version had a limited capability to perfrom self adaption by adjusting the required spring and torsion constants in only one direction. Incorporating either adaptive grid version into the NASJIN code required that the NASJIN code be stopped during the solution proceedure, modify the existing grid to redistribute points in regions where flow gradients are greatest and then restarting the code with this new grid and flowfield. An interface routine was required between the adaptive grid subroutine and the NASJIN code. This necessitated the development of an additional subroutine which would evaluate the transformation metrics for the modified grid.

Alteration of the adaptive grid routine was necessary to make allowances for the additional number of dependent variables computed by the NASJIN code (the specie mass fraction). Coding was added so that each of the flow field variables are determined by interpolation from the modified grid.

Prior to starting this effort, the inclusion of the adaptive grid capability into the NASJIN code was believed to be a simple matter of employing the NASA Ames adaptive grid code as an additional subroutine. The function of this subroutine would be to automatically adjust the required input values. After initiating this effort, it was realized that these constants were highly problem dependent. If incorrect values were used the resulting grid lines would cross. What was believed to be a

simple matter of addition of a few adaptive grid related subroutines became in fact a separate developement effort. The effort required deteriming the appropiate values for the spring and torsion constants for the problem of interest and then modifying the adaptive grid code to adjust these values within specified ranges during the solution of the flow field. It was not possible to accomplish this during the Phase I effort.

A partial success for the adaptive grid code was, however, was obtained. The adaptive grid code was successfully applied to the flow over a bluff base having a centered jet. The freestream conditions utilized were Mach=1.5, 14.7 psi at 520 degrees Rankine. The jet conditions were Mach 1.85, 29.4 psi (exit pressure) at 630 degrees Rankine, the injectant was air. The flow solution was obtained at 500 time steps and a restart tape was written. This restart file along with other required inputs served as input data to the adaptive grid routine and the flow was then solved for another 500 time steps. A plot of the grid at time steps of 500 and 1000 iterations is presented in Figures 2 and 3.

FIGURE 2

ADAPTED GRID AT 500 ITERATIONS

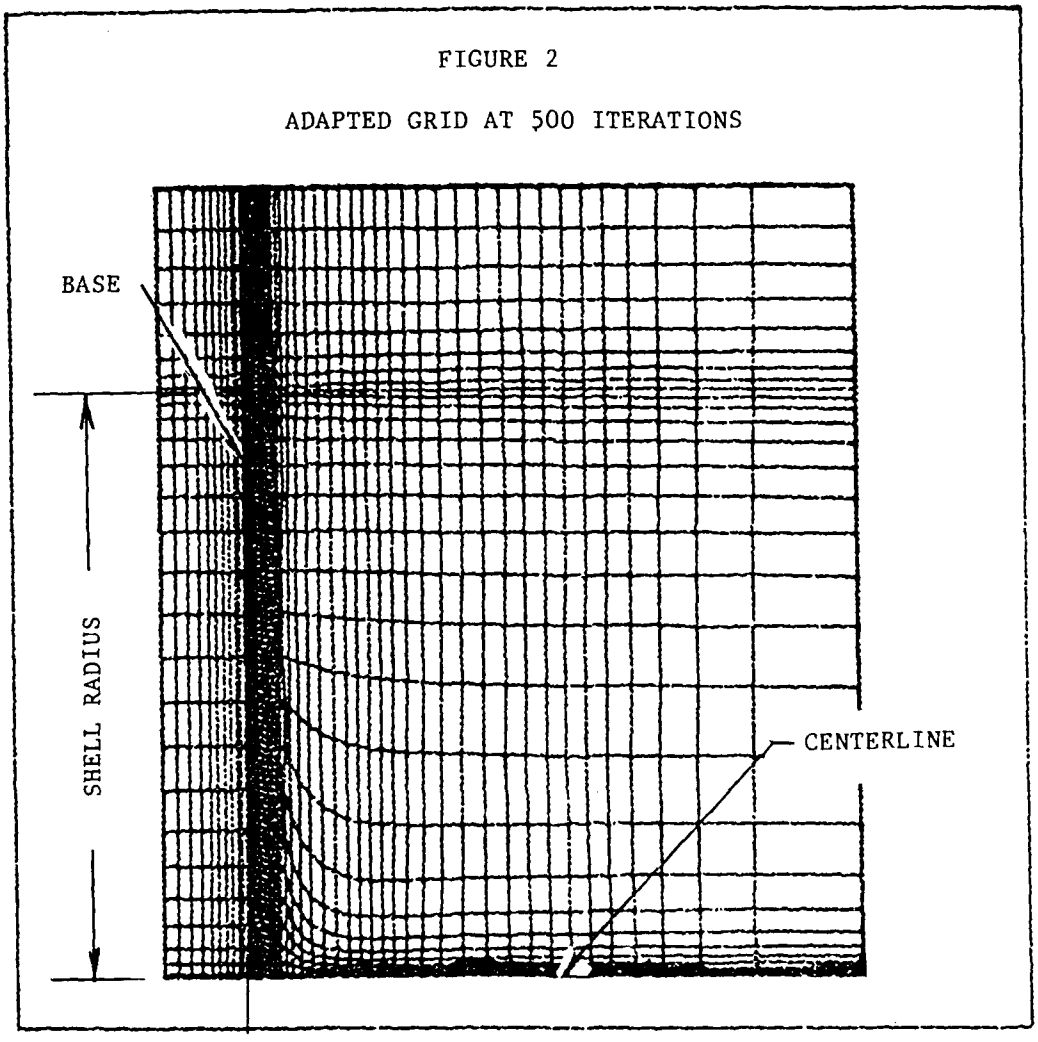

FIGURE 3

ADAPTED GRID AT 1000 ITERATIONS

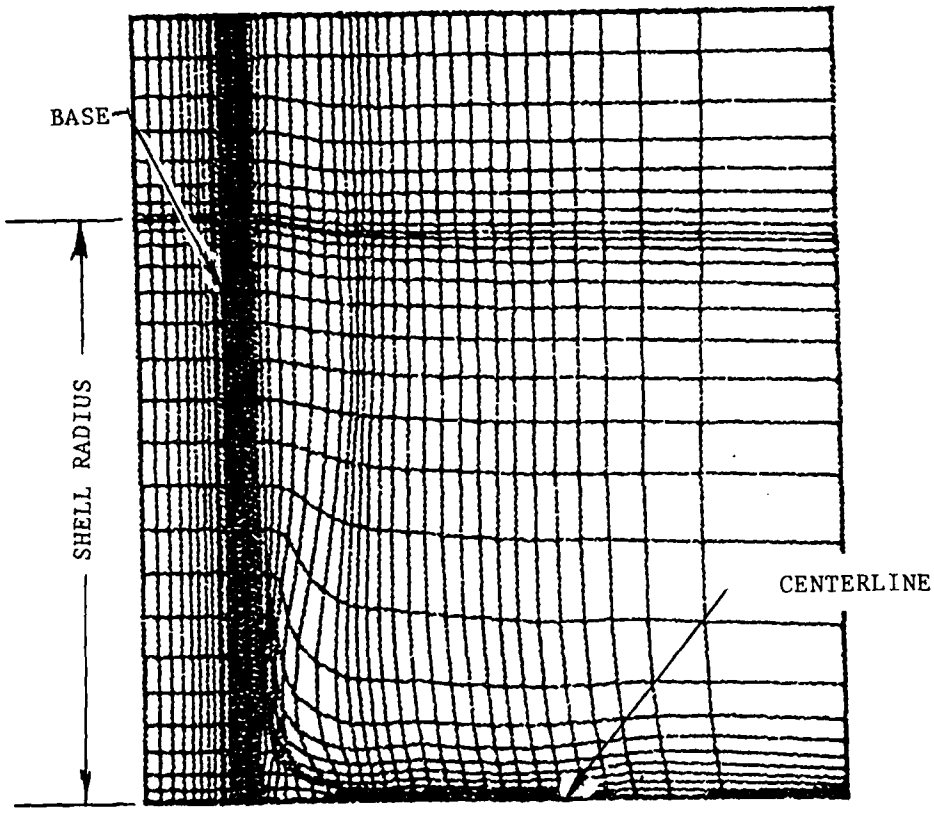

SPIN MODIFICATIONS

Analizing the effects of spin on the base flow was achieved by incorporating additional terms into the two dimensional axisymmetric flow equations. These terms had the effect of imposing an angular velocity everywhere throughout the flow field. This is an approximation and represented an alternative approach to solving the full set of three dimensional flow equations. If the three dimensional flow equations were solved a constant angular velocity boundary condition would have been imposed only on the body surface. Thus the flow field model employed for incorporating spin effects is oversimplified and does not represent the true effects of spin. It does, however, represent a worst case were the spin effects would be exaggerated. A more realistic approach would have been to include a Θ momentum equation and solve for the velocity component in this direction. The three dimensional Navier Stokes equations in a cylindrical co-ordinate system were simplified by neglecting any flow variation in the circumferential direction and assuming a constant spin velocity that is independent of axial location. This simplification leads to the following equations:

continuity:

$$\frac{\partial \rho}{\partial t} + \frac{\partial \rho u}{\partial x} + \frac{\partial \rho v}{\partial y} + \frac{\rho v}{y} = 0$$

x-momentum:

$$\frac{\partial \rho u}{\partial t} + \frac{\partial}{\partial x}\left(\rho u^2 + p + \frac{2}{3}\mu\left(\frac{\partial u}{\partial x} + \frac{\partial v}{\partial y} + \frac{v}{y}\right) - 2\mu\frac{\partial u}{\partial x}\right) + \frac{\partial}{\partial y}\left(\rho uv - \mu\left(\frac{\partial u}{\partial y} + \frac{\partial v}{\partial x}\right)\right) + \frac{\rho uv}{y} - \frac{\mu}{y}\left(\frac{\partial u}{\partial y} + \frac{\partial v}{\partial x}\right) = 0$$

y-momentum $$\frac{\partial \rho v}{\partial t}+\frac{\partial}{\partial x}\left(\rho uv-\mu\left(\frac{\partial u}{\partial y}+\frac{\partial v}{\partial x}\right)\right)+\frac{\partial}{\partial y}\left(\rho v^2+p-\frac{2}{3}\mu\left(\frac{\partial v}{\partial y}-\frac{\partial u}{\partial x}-\frac{v}{y}\right)-2\mu\frac{\partial v}{\partial y}\right)+$$

$$\frac{\rho}{y}\left(v^2-w^2\right)-\frac{2}{y}\mu\left(\frac{\partial v}{\partial y}-\frac{v}{y}\right)=0$$

θ-momentum

$$\frac{\partial}{\partial x}(\rho uw)+\frac{\partial}{\partial y}(\rho vw)+\frac{2}{y}\rho vw=R_\theta$$

where:

$$R_\theta=\frac{\partial}{\partial y}\left(\mu\frac{\partial w}{\partial y}\right)-\frac{\partial}{\partial y}\left(\mu\frac{w}{y}\right)+\frac{2}{y}\left(\mu\frac{\partial w}{\partial y}-\mu\frac{w}{y}\right)$$

The next step is to simplify the θ direction equation and then obtain a suitable functional form for the angular velocity.

Rearranging the terms on the θ equation there is obtained:

$$w\left(\frac{\partial \rho u}{\partial x}+\frac{\partial \rho v}{\partial y}+\frac{\rho v}{y}\right)+\rho v\frac{\partial w}{\partial y}+\rho u\frac{\partial w}{\partial x}+\frac{\rho w v}{y}=R_\theta$$

the first term is zero since it is the steady state continuity equation. This leaves the equation:

$$\rho v\left(\frac{\partial w}{\partial y}+\frac{w}{y}\right)=R_\theta$$

Assuming that the w velocity component is of the form:

$$w = Ay^n$$

and substituting this into the θ equation:

$$\text{rho v } (\text{An } y^{n-1} + Ay^{n-1}) = R_\theta$$

in order for the term on the left side of the equation to be zero n = -1 and A must be a constant. The constant A can be determined using the velocity at the body surface w_b.

$$w_b = \Omega\, y_b = A/y_b$$

where Ω is the angular spin rate. This gives for the value of A:

$$A = \Omega\, y_b^2$$

The end result for the circumferential velocity equation is then:

$$w = \Omega\, y_b^2/y$$

This equation should also be a solution of the viscous RHS of the theta equation. Substituting this into the RHS does in fact indicate that it satisfies the equation. On the centerline this equation is indeterminate, therefore when the vertical co-ordinate is less than the body radius it was assumed that the fluid undergoes solid body rotation. The form for w used in this region is :

$$w = \Omega\, r:$$

Using these forms for the w velocity, at the body surface the w velocity is continuous. The equations used in the NASJIN code employed this w velocity equation to asses the effects of spin on base pressure.

EXPERIMENTAL VERIFICATION

The experimental verification of results predicted by the NASJIN code would serve to establish a confidence level for the code. To accomplish this an experimental program that investigates the effects of base injection location (i.e center or edge injection) and the effects of combustion would be required. A survey was made to determine the availability of wind tunnel facilities where injection tests with combustion could be performed. The objective of the experimental program is to gather detailed flow field data necessary to validate the code. The experiments would be designed to supplement deficiencies in available test data. The primary goal is to define the pertinent flow and geometry parameters which minimize the projectile base drag. A literature survey was performed to determine the extent of existing data relevant to the problem of interest. The survey showed that there is substantial experimental scatter and lack of agreement between prior theoretical models. Also the influence of several important flow parameters such as discrete injection, and model spin is either totally lacking or does not cover a sufficiently wide range of interest. Available test facilities for full scale experiments were examined on the basis of suitability, availability and cost. A list summarizing the results of the available wind tunnel facilities is given in Table

appropiate facilty to perform the tests is that at General Applied Science Laboratories.

Table 1

Test Facilities Contacted

Facility /Location	Test Section	Flow Conditions	Comments	Cost/ Basis
General Applied Science, N.Y.	8"x10"	M = 2.7	Combustion Testing	$9000/wk
Naval Surface Weapons Center Md.	16"x18"	.3<M<5.0	Half Scale No combustion	--
NASA LRC Va.	4'x4'	1.47<M<2.86	No combustion	--
Grumman Aircraft, N.Y.	15"	M = 2.2	Half Scale	--
Wright Aero. Lab., Ohio	8.2"x 8"	M = 3.0	No combustion	2000/day
LTV Texas	4'x4'		No combustion	1375/hr
Rockwell International Ca.	7'x7'	M = 2.0	Some combustion	2800/hr
National Research Council, Can.	5'x5'	.1<M<4.25	Combustion	12500/day
NASA LeRC	1'x1'	1.6<M<5.0	---	---
NASA ARC	6'x6'	1.5<M<2.5	No combustion	---
AEDC APTU	16'x16'	0.0<M<4.5	Combustion	---
New York Univ.	8"x10"	M = 2.7	No combustion	2000/day

PROBLEM GEOMETRY

The geometry employed for the center injection cases is illustrated in Figure 4a and the geometry employed for the edge injection cases is illustrated in Figure 4b. The number of grid points used for each of these configurations is listed in the figure. Typically 100 points were used in the axial direction and 50 grid points in the vertical direction. A cartesian grid was specified with suitable clustering transformations employed to resolve flow details in the vicinity of the corner and injector areas.

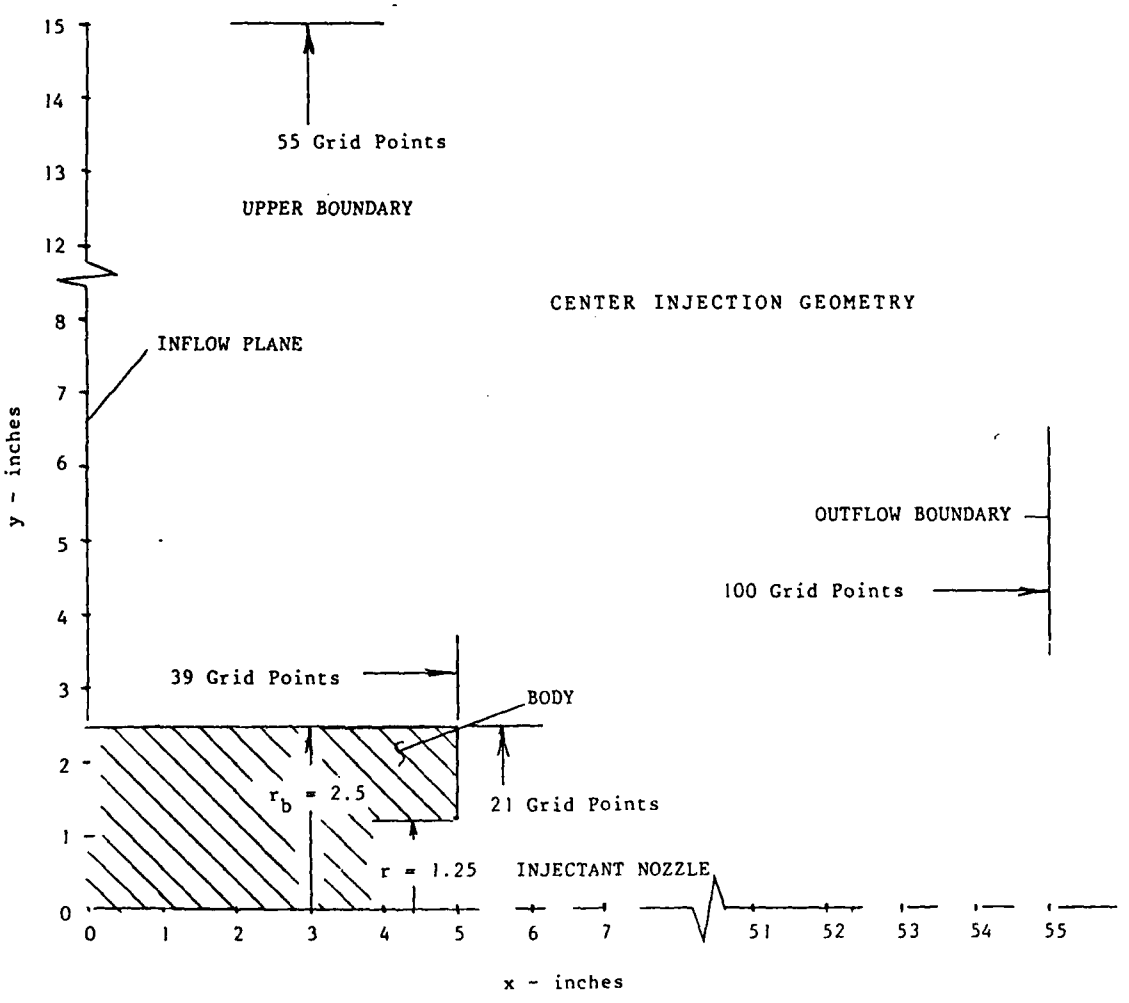

CENTER INJECTION GEOMETRY
FIGURE 4a

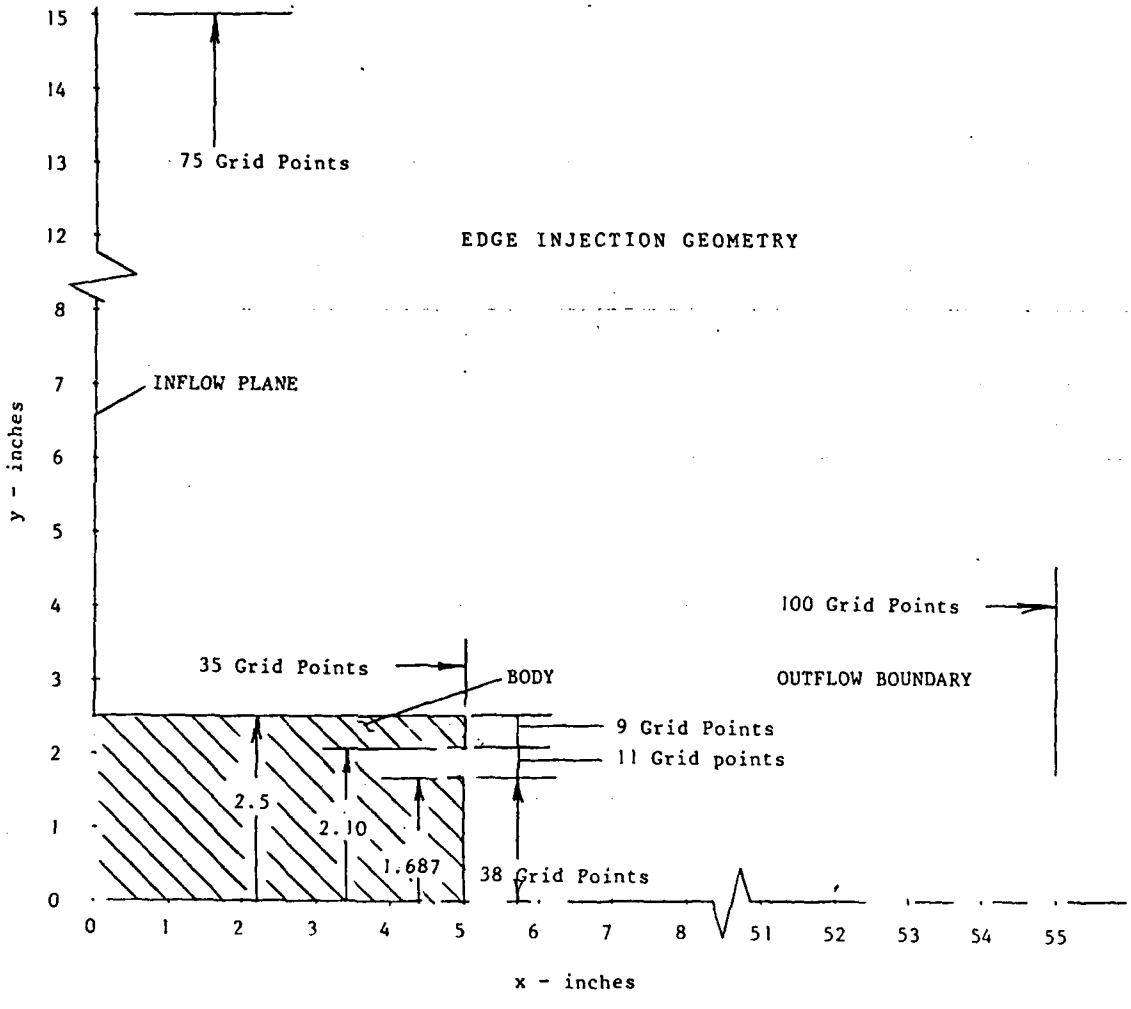

EDGE INJECTION GEOMETRY
FIGURE 4b

DESCRIPTION OF THE COMPUTER CODE

the computer code used to perform the parametric studies is termed NASJIN which is an acronym for Navier Stokes Jet INjection. The equations employed in the code are the two dimensional axisymmetric unsteady two specie Navier Stokes equations. These equations are given below:

$$\frac{\partial U}{\partial t} + \frac{\partial F}{\partial x} + \frac{1}{r^n}\frac{\partial (r^n G)}{\partial r} + n\frac{H}{r} = 0$$

n=0 Two Dimensional Flow
n=1 Axi-symmetric Flow

$$U = \begin{Bmatrix} \rho \\ \rho u \\ \rho v \\ \rho e \\ \rho f \end{Bmatrix} \qquad G = \begin{Bmatrix} \rho v \\ \rho uv + \tau_{xr} \\ \rho v^2 + \sigma_{rr} \\ (\rho e + \sigma_{rr})v + \tau_{xr}u + \dot{q}_y \\ \rho vf + \dot{m}_y \end{Bmatrix}$$

$$F = \begin{Bmatrix} \rho u \\ \rho u^2 + \sigma_{xx} \\ \rho uv + \tau_{xr} \\ (\rho e + \sigma_{xx})u + \tau_{xr}v + \dot{q}_x \\ \rho uf + \dot{m}_x \end{Bmatrix} \qquad H = \begin{Bmatrix} 0 \\ 0 \\ -\sigma_{\theta\theta} \\ 0 \\ 0 \end{Bmatrix}$$

where

ρ = density
u = axial velocity
v = vertical velocity
e = internal energy
f = specie mas fraction
m = mass fraction rate of change
$\tau_{xr}, \tau_{xx}, \sigma_{xx}, \sigma_{rr}, \sigma_{\theta\theta}$ = stress components

This code has evolved over a number of years and is based on work performed in references 4,5 and 6. The equations are solved using the explicit technique of MacCormack (7). There are five independent variables which are solved for, the density, x velocity, y velocity, total energy and the specie mass fraction. The flow is not considered to have a constant total temperature. Therefore at the inflow plane or base injection plane the static temperature is specified as a function of y. This results in a total temperature and therefore a total energy variation in the vertical direction.

CODE MODIFICATIONS

A significant modification that was required to the code was implementing a subsonic inflow boundary condition for the injected mass. This was done using an additional subroutine. Two approaches were tried, the first was to assume a total injection pressure that was only slightly larger than the static pressure in the base region. Using these two pressures the injectant Mach number was then computed. The injectant mass flow ratio "I" was specified and also the injectant total temperature. Using the total temperature and the Mach number the injectant static temperature and velocity was then computed. Using the static pressure and the static temperature the injectant density was then calculated. An estimate for the mass injectant flow rate ratio "I_p" was then computed using the velocity, density and injectant area. This value was then compared to the specfied injectant mass flow rate value. The first value was always less than the specfied value (the initial value for the injectant total pressure was chosen so that this was always the case). The injectant pressure was then increased gradually until the calculated value for the mass injection was greater than the specified value. The correct value for the injectant conditions was then interpolated on. These values were then used to compute a new estimate for the mass injectant parameter. If the two values agreed to within 2%, the iteration was stopped, if not the total pressure increment for the injectant was decreased and the process was started over again. This approach appeared to work until at about 9000 iterations it broke down. Large values of base pressure were obtained. The reason for the occurence was not resolved. Because of this a second approach was also pursued.

The second approach was to express the mass flow as a function of the injectant conditions using the expression for the injection mass flow ratio.

$$I = \frac{(\rho u A)_j}{\rho_\infty u_\infty A_b}$$

Using the equation for a perfect gas, the definition of the Mach number, and speed of sound an expression for the injectant Mach number can be obtained.

$$M_j = I \frac{\rho_\infty u_\infty}{p_j} \frac{}{A_j} \left(\frac{RT}{\gamma}\right)_j^{1/2} A_b$$

Note: The pressure used in this equation was an average pressure at the first flow field interior grid point over the injectant exit area.

This expression is solved for the Mach Number using an iteration process. A value for the injectant total temperature is specified and assumed to be constant. An estimate for the injectant static temperature ($T_j = T_{\infty j}$) is assumed. The above expression is used to compute the Mach number. The static temperature is updated using the new value of Mach Number. A second value for the Mach Number is determined and compared to the first. This process is repeated until there is no change in the value for the Mach Number. Typically this required 8 iterations. After the Mach Number is determined the static temperature is computed, the injectant velocity and then the injectant density. This second approach was successful.

The second routine that was added to the code was one that computes the force on the projectile base. The integration of the base pressure used a simple trapezoidel integration technique. Separate values for the static force and injectant momentum were computed. The injectant momentum force is not include in the base force results and would contribute an additional 10% to the base force for injectant values greater than I=.04.

In addition to the above two modifications to the computer code a major restructuring of the code was performed. This major restructuring was to replace all the double array subscripted variables with a single array. The effect of this is to increase the vector length. During the process of performing the code restructuring any coding that inhibited do loop vectorization was removed from the loop.

The major differences between the two versions of the code are that the single array version has no 'IF' statements inside the inner DO loops and has a vector length of NNX (number of points in the x direction) times NNY (number of points in the y direction). For example for a 100 (NNX) by 50 (NNY) grid the old version had a maximum vector length of 100 (the x dimension length). The new version now has a vector length of 1500 (NNX*NNY). This allows use of the maximum length vector permitted by the CRAY processors.

The changes to the code where made on the IBM AT. The code was then was compiled on the IBM PC AT to locate and correct any FORTRAN syntax errors. Typically it took about 20 minutes to compile the 4500 lines of code on the IBM AT. The code was then loaded onto the CDC CYBERNET system and benchmarks between the old version and the new single array version were made. The results from the single array version were compared to results from a previous version of the code. Both sets of results were in agreement indicating that there were no coding errors introduced as a result of the code changes.

The results of these benchmarks are given in Table 2. Typically the new single array version runs about three times faster on the Cray XM/P and three times faster on the CYBER 205. This new version of the code does not have the subsonic injection boundary condition routine or the base force routine.

Table 2

Benchmark Comparison
(Performed on CDC Cybernet System)

CPU Execution Time in Seconds

Version / Computer	Original Code	Single Array	Optimized Single Array
CYBER 205	337.6	110.1	----
CRAY X-MP/24	80-90*	46.85	28.6

(These times do not include compilation time)

CPU Breakdown on Cray X-MP/24

Routine	Single Array	Optimized Single Array
NASJIN	1.246	1.209
TRAN	.120	.116
THERMD	4.667	.964
BC	2.690	2.634
SIDE	.873	.861
STP	16.560	3.450
SOLVR	8.030	8.116
SMOOTH	4.044	3.239
STRESS	5.446	5.166
FLUXES	2.180	1.916
PRINT	.905	.868
Other	.089	.061
Total CPU time (seconds)	46.85	28.6

Benchmark case was a 60x40 grid run for 1000 time steps

* Estimated: The original version required 139 seconds on a CRAY-1 S/2000. The CRAY X-MP/24 was not avaiable for this original benchmark.

COMBUSTION MODEL

The Phase I effort considered the effects of combustion by employing a flame sheet hydrogen air combustion model (8). In this type of combustion model the chemical kinetics employed are those of chemical equilibrium or an infinitely fast chemical reaction. This is a useful model of a single constituent fuel combustion process that is essentially a simplified treatment of local chemical equilibrium. This identical approach has been employed in references 5 and 6 for analysis of a hydrogen fueled scramjet combustor. The model can be illustrated by considering a hydrogen air system. Restricting the treatment to problems with a maximum temperature of less than 2500°K, an examination of the pertinent equilibrium constants reveals that it is reasonable to neglect all reactions involving nitrogen and that the existence of the radicals of oxygen and hydrogen (i.e., O, H and OH) can be neglected. Thus, only the simple overall reaction

$$H_2 + 1/2\ O_2 \rightleftharpoons H_2O$$

with the related equilibrium constant

$$K_{p,3} = \frac{P_{H_2O}}{P_{H_2} P_{O_2}^{1/2}}$$

must be considered. Furthermore, for T < 2500° K, $K_{p,3} \gg 1$, so it can be asserted that either the concentration of hydrogen or oxygen must be essentially zero in certain regions of the flow. Thus, we come to the flame sheet model where the flow is divided into two regions: one where there is no fuel and one where there is no oxygen. The boundary between the two is the "flame sheet" where the concentration of both hydrogen and oxygen is zero. This "flame sheet" occurs at the locus of points where the ratio of oxygen atoms to hydrogen atoms is stoichiometric. This model is illustrated in Figure 5.

The flame sheet model is an equilibrium chemistry model. Therefore, a flame sheet dynamic equilibrium combustion model can be considered to be an extreme case where the highest degree of heat release is obtained both from a chemical kinetics and fluid dynamics model. This would then represent one extreme for the flow phenomena under investigation.

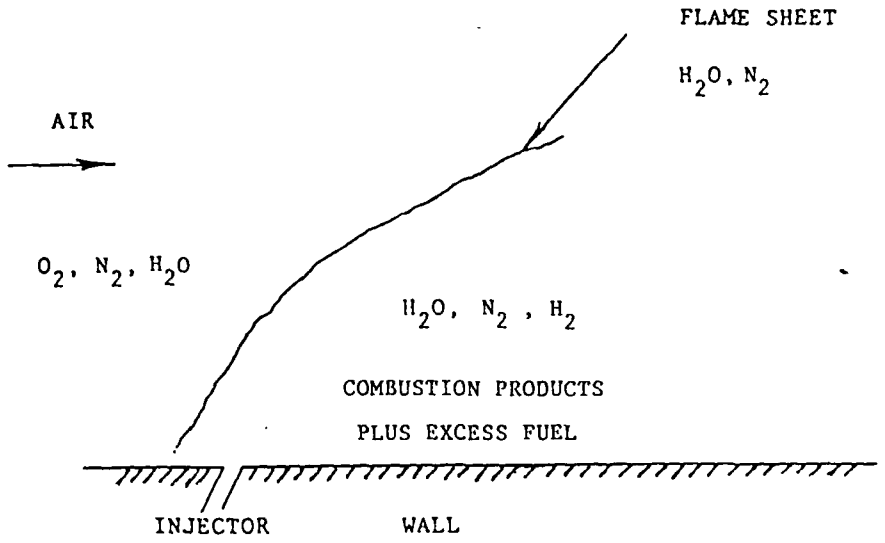

FLAME SHEET SCHEMATIC

FIGURE 5

The method of solution for the flame sheet model model is to first compute the flow field fluid dynamics for a single time step. This determines the amount of fuel that is diffused and convected by the flow field during this time step. Next the amount of oxygen and nitrogen present at each grid point is determined. This is done using the relations:

$$Y_{O2} = (1.0-Y_{H2}) * .232 \quad \text{and} \quad Y_{N2} = 1.0-Y_{H2}-Y_{O2}$$

The .232 value in the above relation is the gram atom weight of oxygen present in the amount of air and is determined by the following calculation:

Gram atom weight of air = W_a

W_a = Number of oxygen atoms x oxygen atomic weight +
Number of nitrogen atoms x nitrogen atomic weight x
number of nitrogen atoms for each atom of oxygen

$$= 2 \times (16) + 2 \times 14.0 \times 3.76 = 137.28$$

$$W_{O2}/W_a = 32/137.28 = .232$$

The local stoichiometric ratio at each grid point is determined based on the local hydrogen and oxygen composition:

$$Y_s = (2.016/16.00)\ Y_{O2}$$

A comparison is made to determine if the amount of hydrogen present is greater or less than Y_s. If the amount of hydrogen

present is greater than the stoichiometric value the amount of hydrogen consumed in the reaction is set equal to the stoichiometric value. The residual amount of hydrogen is then:

$$(Y_{H2})_{final} = (Y_{H2})_{initial} - Y_S$$

If the amount of hydrogen present is less than the stoichiometric value then all of the hydrogen is consumed in the reaction and

$$(Y_{H2})_{final} = 0.0$$

In the case when there is excess hydrogen, the amount of oxygen and water are computed from the equation:

$$(Y_{O2})_{final} = (Y_{O_2})_{initial} - 16.0*Y_S/2.016$$

$$(Y_{H2O})_{final} = 18.016 * Y_S/2.016$$

or for the case when there is not enough hydrogen for complete combustion

$$(Y_{O2})_{final} = (Y_{O2})_{initial} - 16.0*Y_{H2}/2.016$$

$$(Y_{H2O})_{final} = 18.016 * Y_{H2}/2.016$$

The results of the above proceedure allow computing the gas composition at each grid point. This composition is then used to compute the static enthalpy of the mixture. The enthalpy is then used in the equation for total energy to compute a new value of temperature after the fuel and air has burned.

PARAMETRIC CASES

The effects that were investigated consisted of determining the impact on base drag of:

1) edge injection in the axial direction
2) center injection in the axial direction
3) edge injection at an angle of 45°
4) effect of injectant temperature
5) effect of spin
6) air and hydrogen injection with no reaction
7) air and hydrogen injection with reaction

The effect of injectant conditions on the injection mass flow requirements was estimated as a function of free stream Mach Number. Results of these calculations are shown in Figures 6, 7 and 8. These curves were generated only to obtain a relative comparison of different conditions. It was assumed for all of these cases that the base pressure was constant and equal to 7.0 psia and the base area to injectant area ratio was constant at a value of 2.5. The figures indicate that the higher the injectant temperature and molecular weight the lower the injectant mass flow requirements to obtain the same value of base pressure.

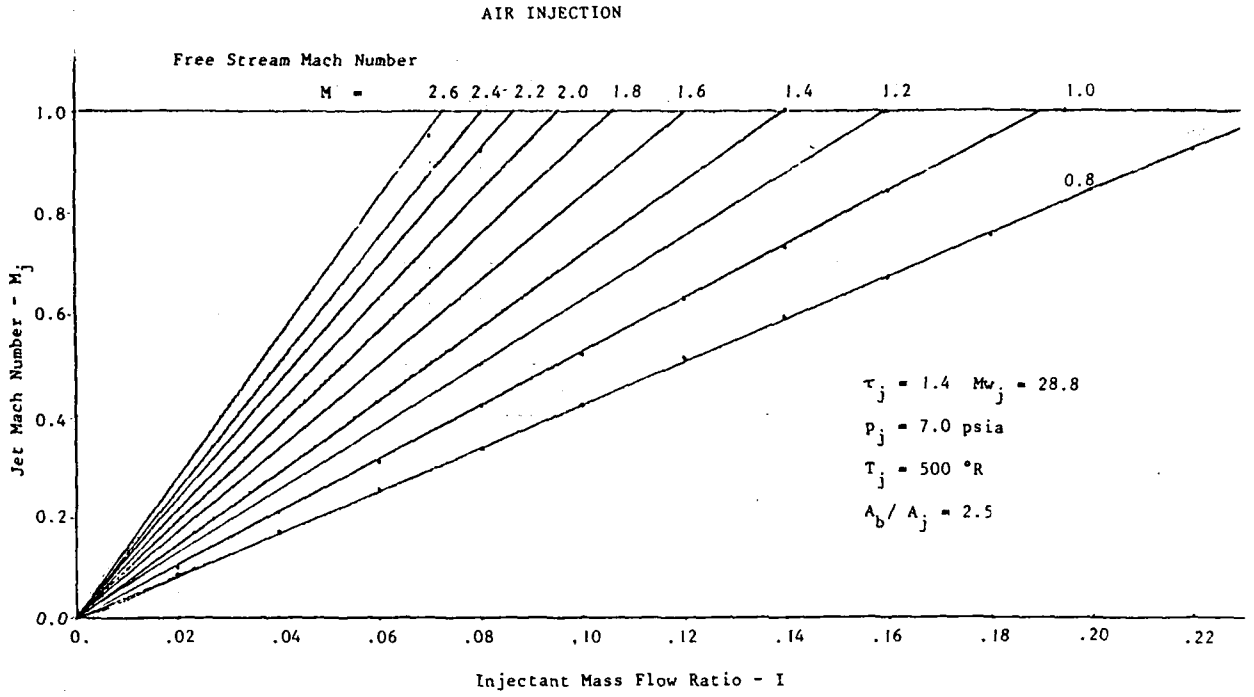

AIR INJECTION

FIGURE 6

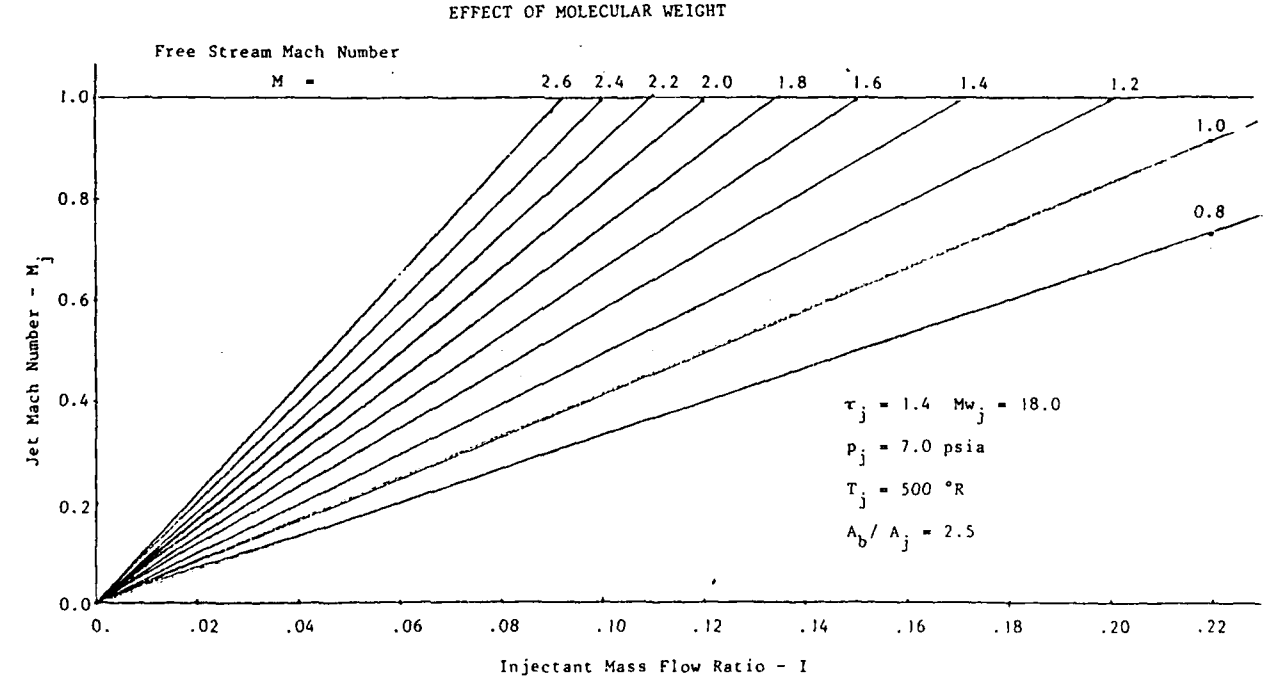

EFFECT OF MOLECULAR WEIGHT

FIGURE 7

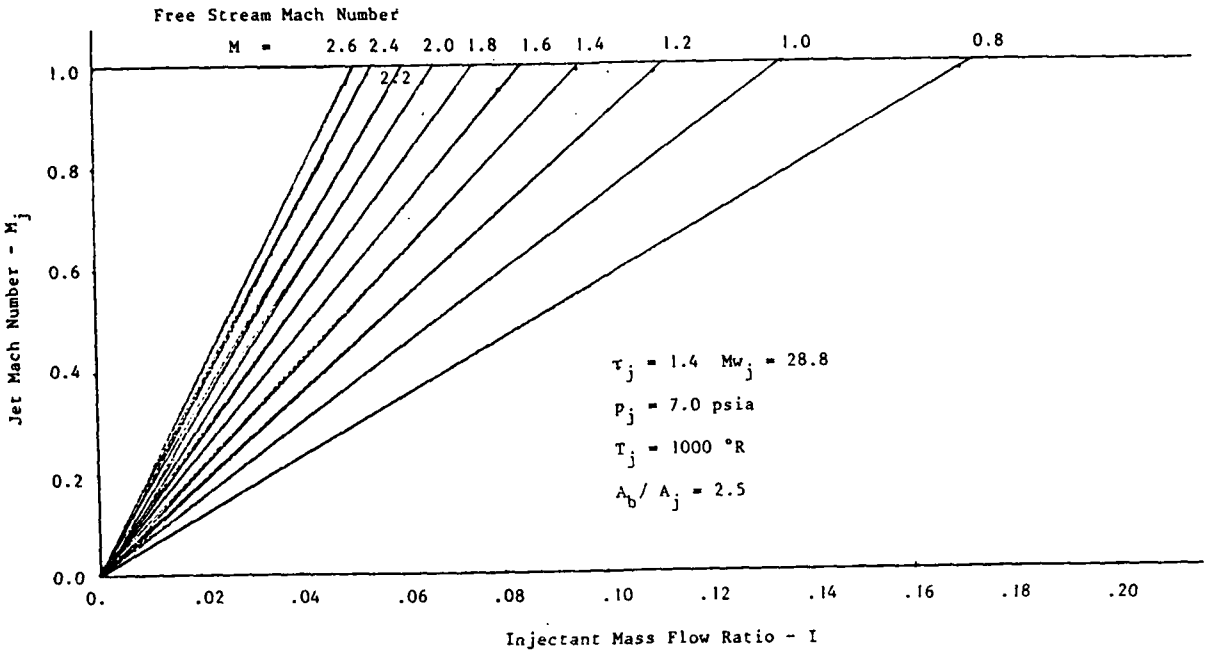

EFFECT OF TEMPERATURE

FIGURE 8

THEORETICAL RESULTS

The majority of the theoretical results obtained from the NASJIN code were performed on the Ballistic Research Laboratory CRAY XMP/48. The computer was accessed over a toll free dial in line at 1200 baud. Typical run times using the original version of the code required 30 minutes to 90 minutes depending on the number of grid points and the number of time steps. The 90 minute run typically was for 20,000 time steps using a grid with 100 points in the x direction and 55 grid points in the y direction. The turn around time was either overnight or if a job was submitted early in the day it would be finished by late afternoon.

The theoretical effort performed focused on determining the effects of central injection and edge injection on projectile base drag. Prior to performing the injection studies, it was desirable to correlate the results of the code with experimental data when there was no base injection. The computed base pressure with no injection are plotted in Figure 9. Also shown in the figure are experimental results from NACA report 1051 "An Analysis of Base Pressure at Supersonic Velocities and Comparison with Experiment" by Dean R. Chapman. The computed values of base pressure agree to within 10% of the experimental values. The base pressures with no injection from AIAA Paper 86-0487 "Supersonic Flow over Cylindrical Afterbodies with Base Bleed" by J. Sahu are also shown on the figure. Again these values agree to within 10% of the experimental values. The original data from NACA 1051 is shown in Figure 10 and covers a wide range of experimental test conditions and body configurations. Therefore agreement to within 10% is not unreasonable.

Having established a confidence level of the code when there is no injection, the objective was to determine the confidence level of the code with injection. The base pressures for cases

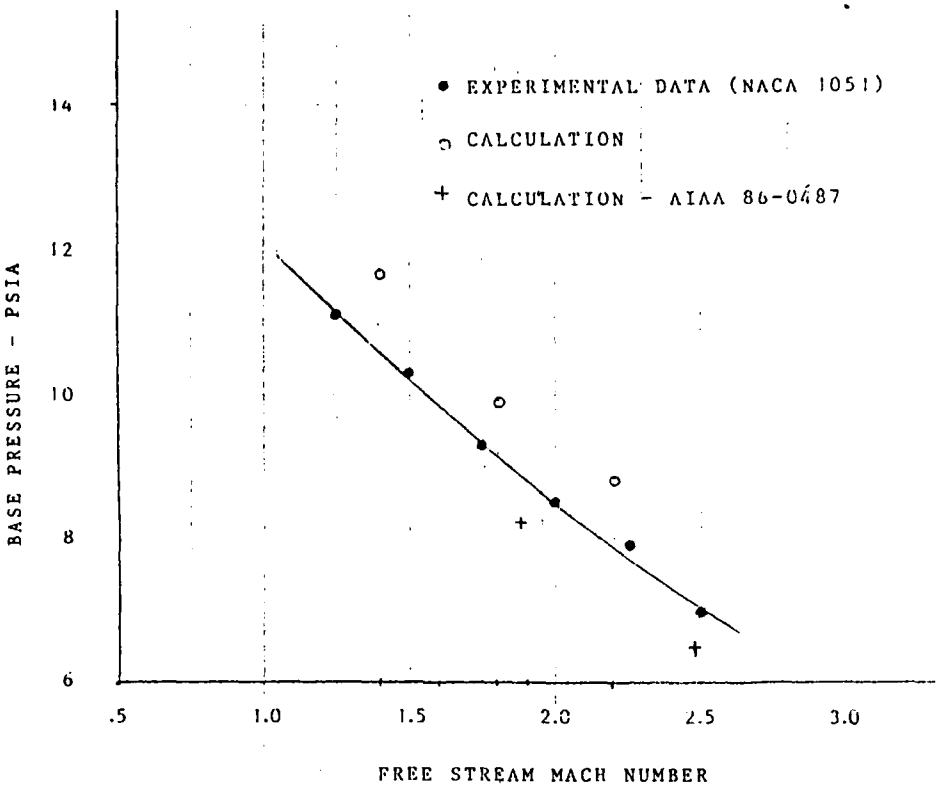

BASE PRESSURE VERSUS MACH NUMBER

FIGURE 9

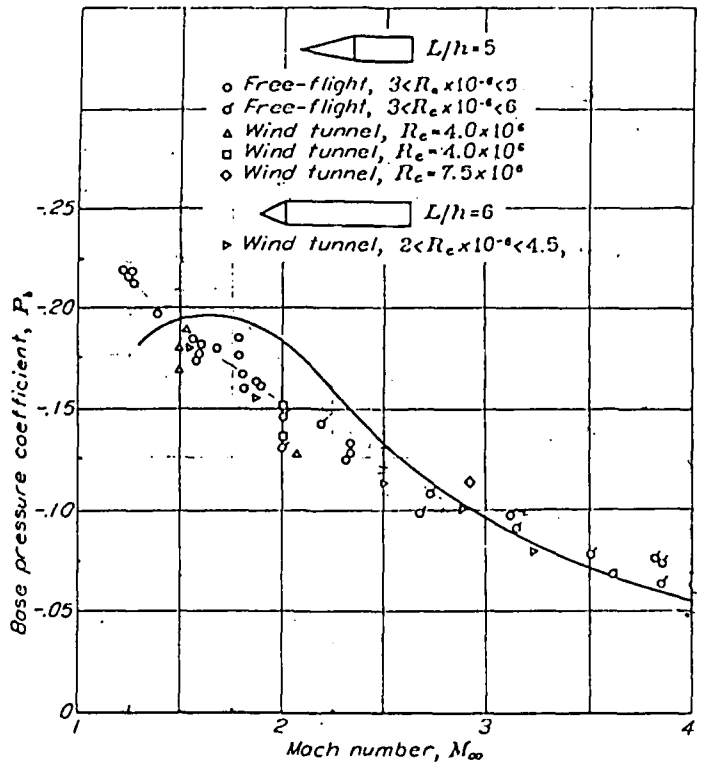

VARIATION OF BASE PRESSURE COEFFICIENT WITH MACH NUMBER

FIGURE 10

with injection again from AIAA Paper 86-0487 "Supersonic Flow over Cylindrical Afterbodies with Base Bleed" are shown in Figure 11. The results are for a Mach 1.8 center injection case whereas the AIAA results are for a Mach nunber of 1.7. Although the body sizes and free stream conditions are not the same for these two cases there is general agreement between the two sets of results. The minor difference between the current calculations and the previous ones is that there is no minimum value for base drag as the injection mass ratio "I" increases. The base drag continues to decrease as injection increases, indicating the more mass injected the lower the base drag.

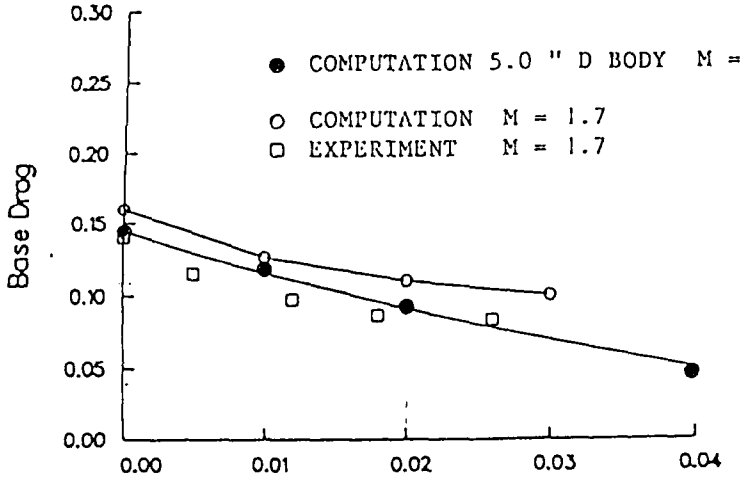

BASE DRAG VERSUS MASS INJECTION RATIO

FIGURE 11

Parametric calculations were then performed for center and edge injection on the 5.0 inch diameter body of Figure 4. Results for air injection are shown in Figure 12 for central injection and Figure 13 for edge injection. Injectant total temperature for these cases was the same as the free stream total temperature. Both the value of the force and the base drag coeffficinet are plotted in the figures. In general for center injection, as the amount of mass injection increases the base drag decreases. This is true for both central and edge injection. An exception to this is the center injection Mach 1.4 case which exhibits a definite peak at I=.03. The edge injection results, however, indicate that at the lower Mach number of 1.4 a substantial drag reduction occurs with only a small amount of mass injection (I=.01). In fact the edge injection actually results in forces large enough to generate some degree of thrust. As the free stream Mach number increases the base drag coefficient decreases but is still large enough so that there is almost no base drag penalty incurred. In general the edge injection results indicate a potential improvement in projectile range may be obtained over that of central injection. To determine the degree of improvement requires performing trajectory simulations for the different injection techniques.

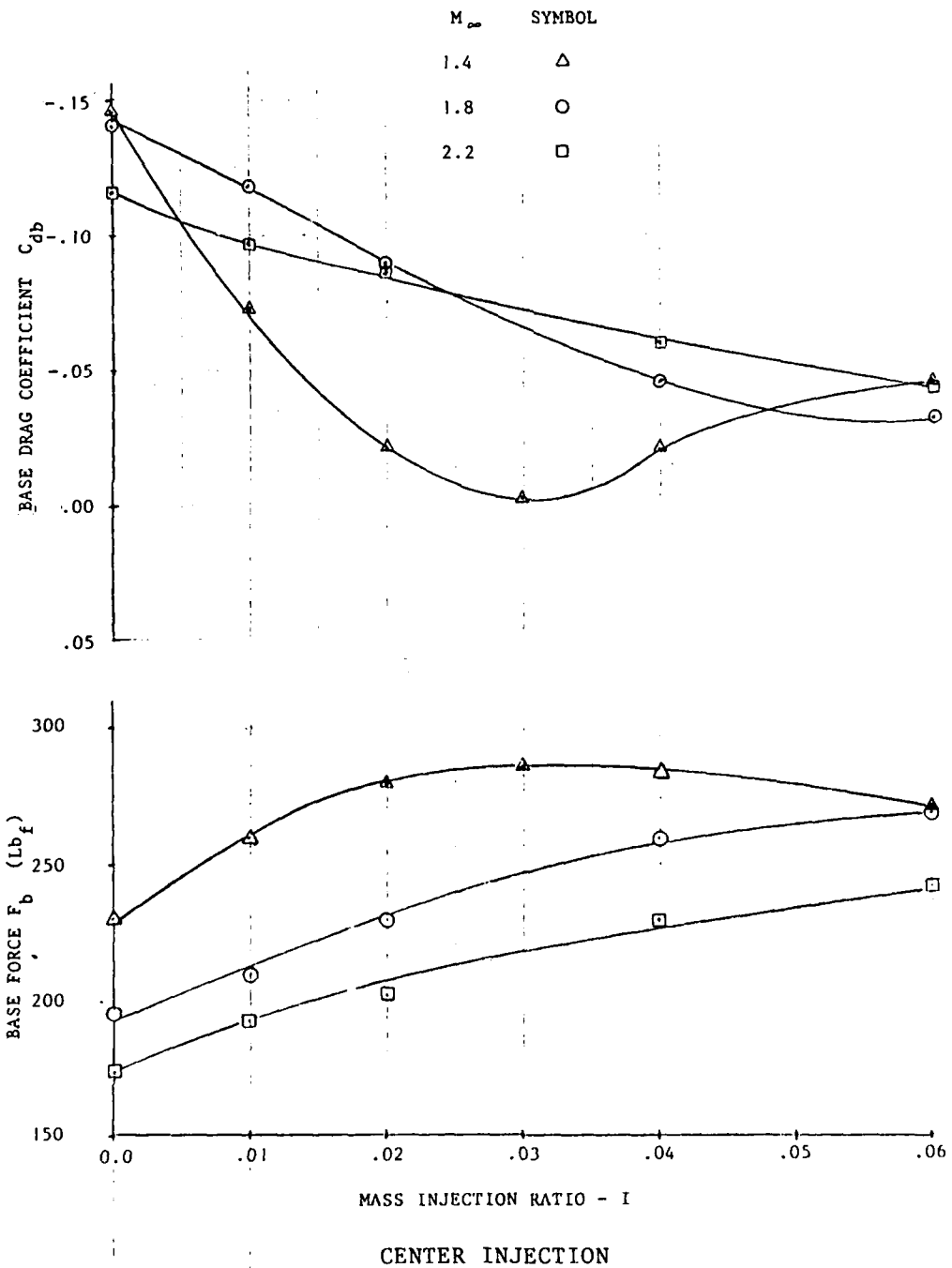

CENTER INJECTION
FIGURE 12

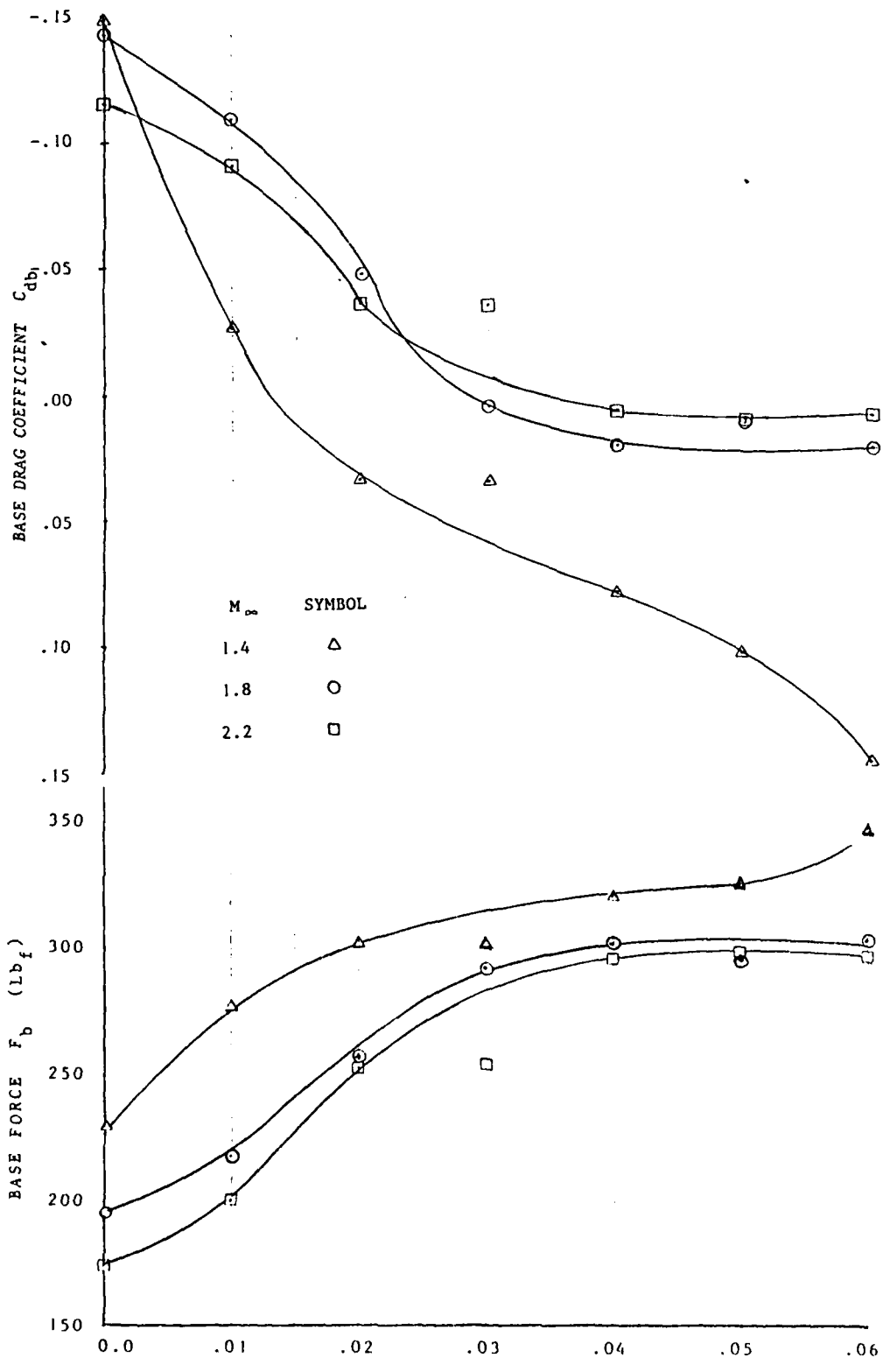

EDGE INJECTION

FIGURE 13

A possible explanation of this is that edge injection is more effective in generating an equivalent streamlined body then center injection. This is depicted in Figure 14a and 14b. For the same amount of mass flow the center jet injectant has to spread further than the edge jet injectant to attenuate the expansion of the free stream gas into the centerline region of the body. Therefore, based on these initial results, it appears that edge injection is more effective in the reduction of base drag then central injection. These results however should be verified by additional calculations and experimental wind tunnel tests.

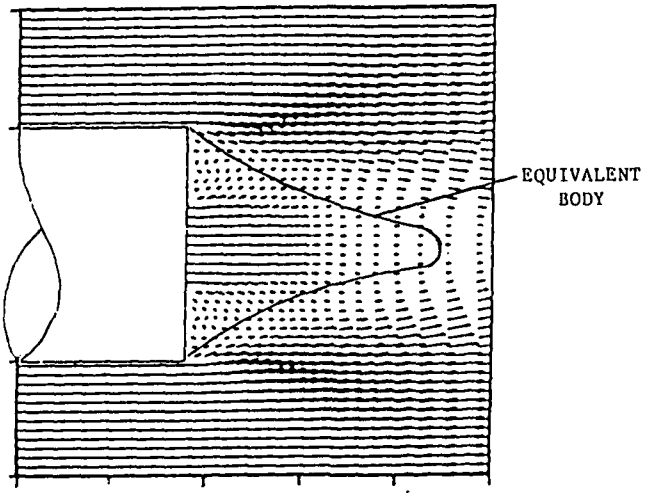

CENTER INJECTION

FIGURE 14a

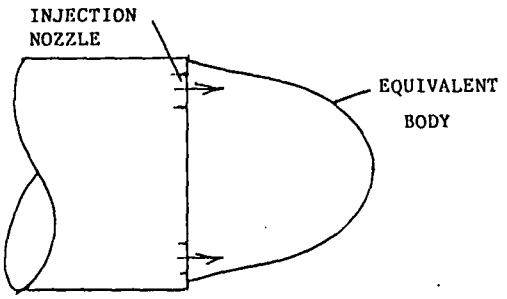

EDGE INJECTION

FIGURE 14b

EQUIVALENT BODY CONFIGURATIONS

FIGURE 14

The effect of injection angle angle for the edge injection case was also investigated. Shown in Figure 15 are the results for injecting at an angle of +45° and -45°. The results indicate that angled injection in general detracts from the reducing the base drag. There is also a crossover where a negative injection angle is initially better than positive injection until at an injection ratio of I=.04 where this trend is reversed. The reason for lookin at this effect was based on the fact that if the injectant was directed at an angle of 45° up into the oncoming free stream flow, it would appear as blockage to this incoming stream and cause an increase in the projectile lip pressure which would in turn cause an increase in the base pressure. To fully study this effect a three dimensional computer code is required that would be capable of analyzing discreet injection. The area between the discrete injector orifices would allow the higher projectile lip pressure to be communicated into the base region, thereby increasing base pressure and decreasing base drag.

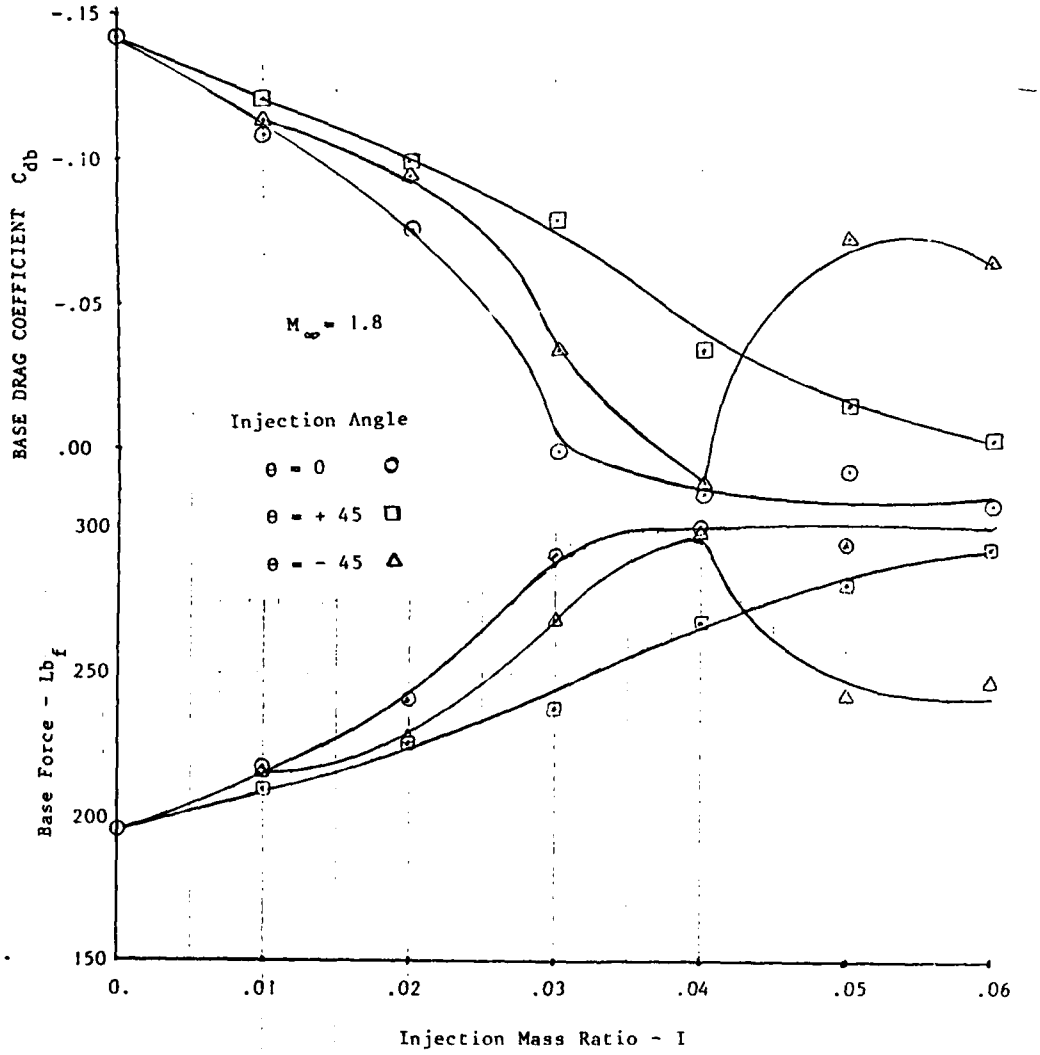

EDGE INJECTION EFFECT OF ANGLED INJECTION

FIGURE 15

The effect of injectant temperature was then investigated at a free stream Mach number of 1.8. The injectant temperature was increased to 1100° R from 854° R. At the injectant plane (the base region station) the injectant static temperature is specified and does not have to be equal to the free stream static temperature. This difference in static temperature at the injectant plane also gives rise to a variation in the total energy between the external stream and the injectant. The results of these calculations are shown in Figure 16. In contrast to the previous cases where the injectant total temperature was equal to the free stream total temperature, there is now a more distinct optimum injectant mass flow rate that occurs at I = .03. The effect of increased injectant temperature gives a further reduction in base drag than cold air injection.

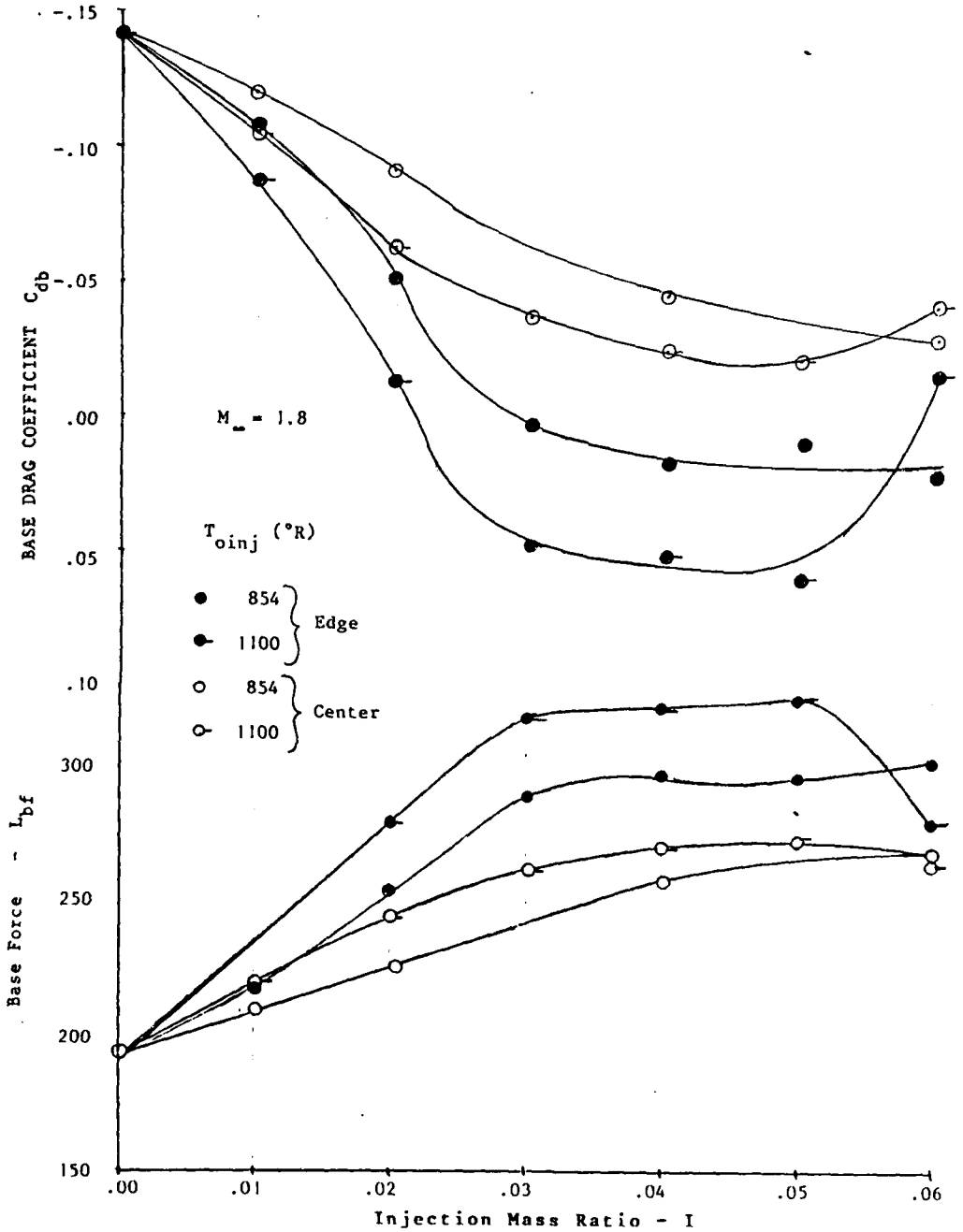

EFFECT OF INJECTION TEMPERATURE

FIGURE 16

The effects of spin on central injection is illustrated in Figure 17 and for edge injection in Figure 18. The spin rates were 20,000 rpm and 30,000 rpm for the center injection case and 10,000 and 20,000 rpm for the edge injection case. Spin causes a lowering of the base pressure as is shown in the figures, apparently the spin imparts a radial outward velocity to the gas in the base region. This decreases the density of the base region gas and therefore also the base pressure. The central injection shows a monotonic variation of the base force with spin. The effect of spin on edge injection is to decrease the erratic behavior that occurs with no spin.

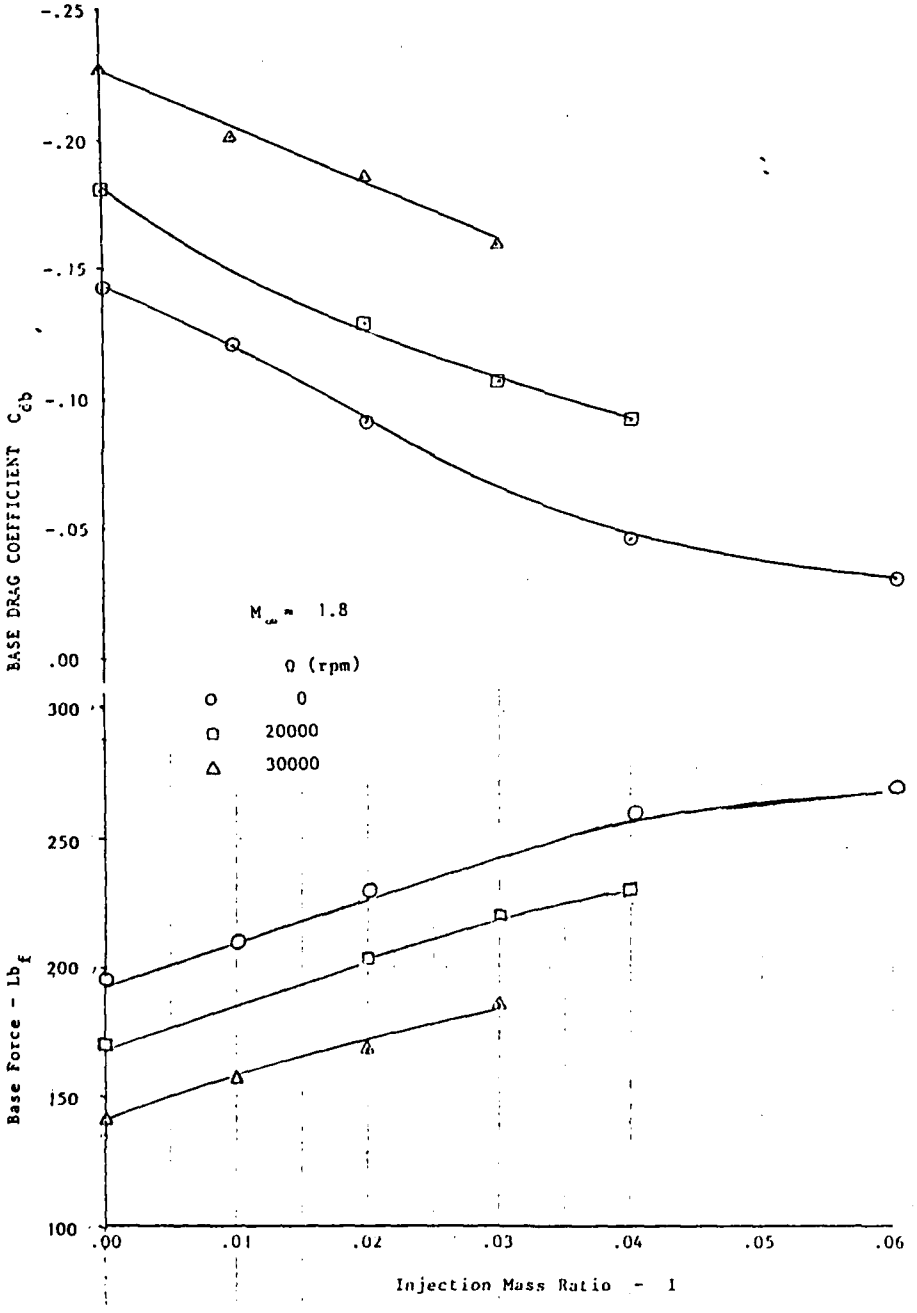

EFFECT OF SPIN CENTER INJECTION

FIGURE 17

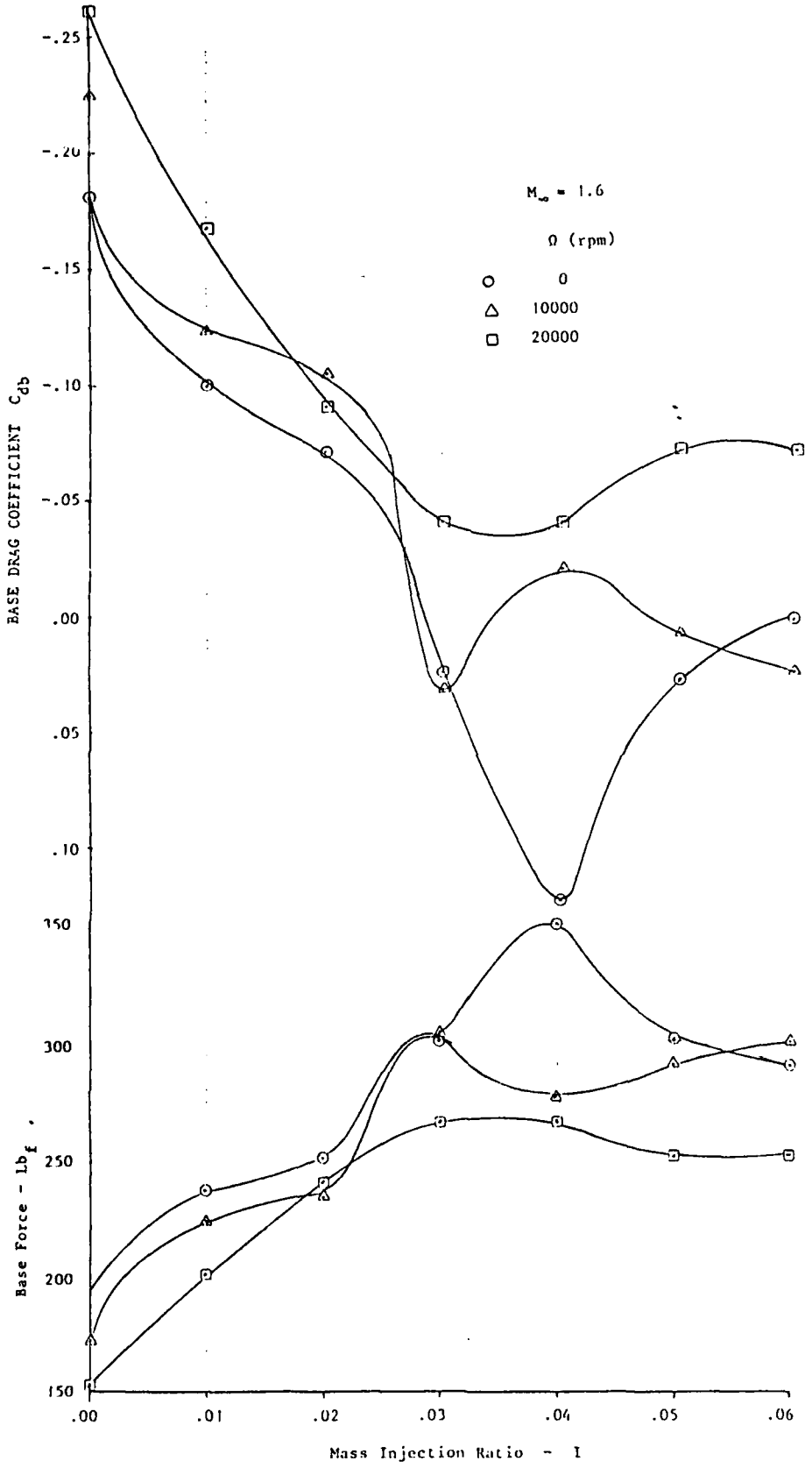

EFFECT OF SPIN EDGE INJECTION

FIGURE 18

The effects of injecting a mixture of hydrogen and air for the center injection case is shown in Figure 19 and for the edge case in Figure 20. The amount of hydrogen that was injected is a mass fraction of .007. Although this may seem small the hydrogen mass fraction for a stoichiometric air hydrogen mixture is .027. Thus the amount of hydrogen injected is about one fourth the stiochiometric value. This value was choosen to avoid an excessive amount of heat release that may cause the code to go unstable. The results in the figures indicate that the hydrogen causes the base force to increase and base drag to decrease. This agrees with other published work which indicates that the injection of light molecular weight gases in the base region are more effective in decreasing base drag.

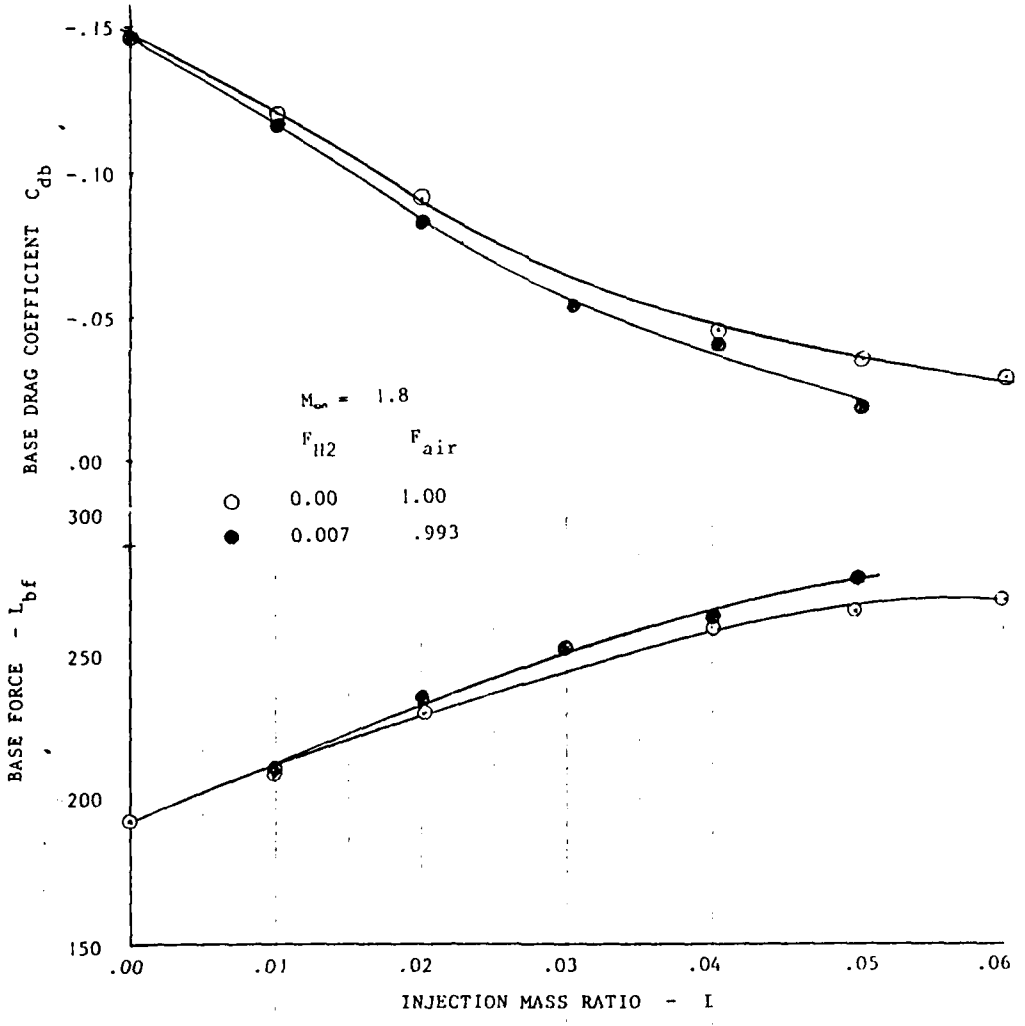

CENTER INJECTION WITH HYDROGEN

FIGURE 19

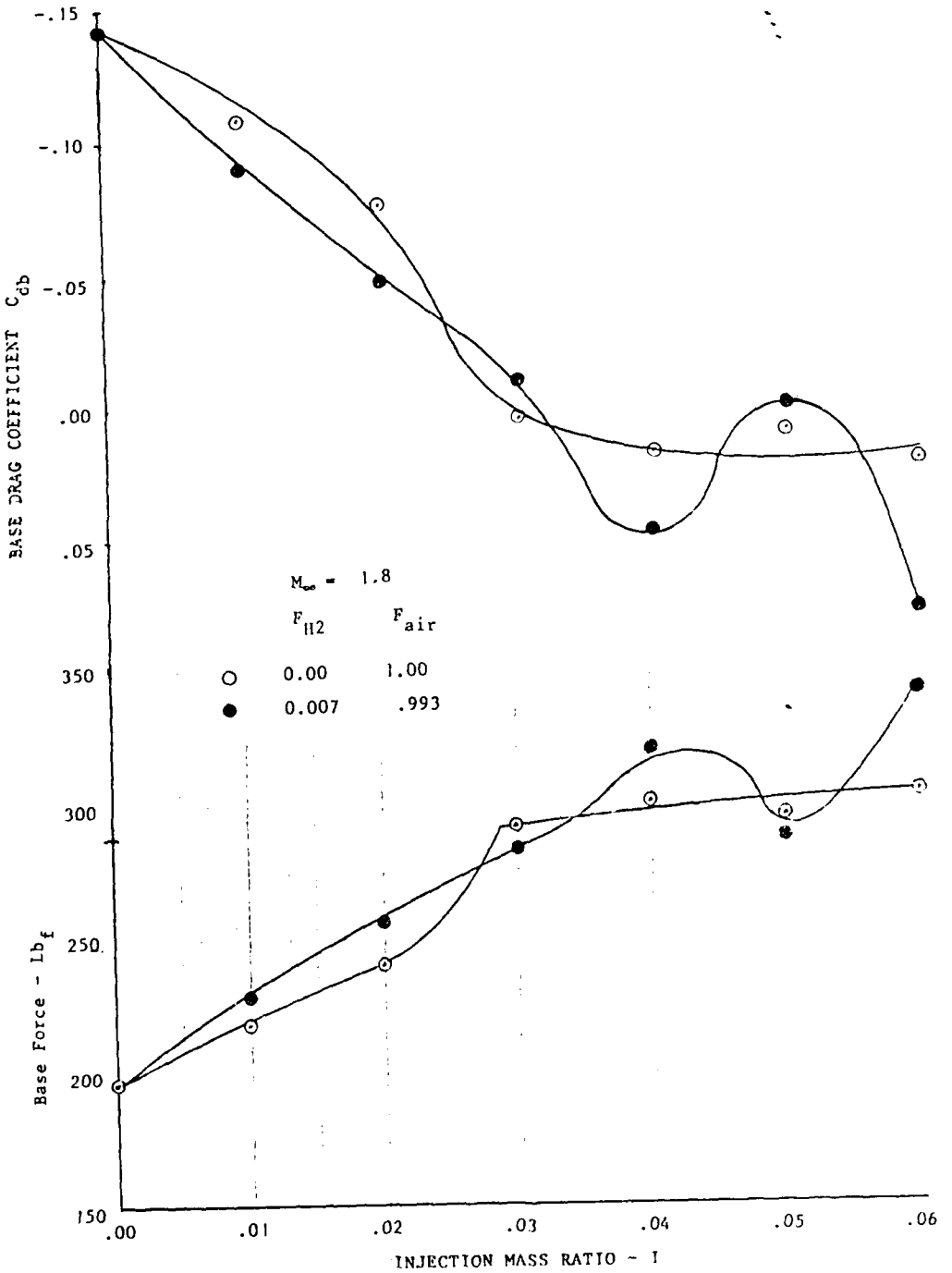

EDGE INJECTION WITH HYDROGEN

FIGURE 20

The effects of combustion in the base region is shown in Figure 21 for the edge injection case. The amount of hydrogen that was injected is the same as in the previous case (hydrogen mass fraction = .007). The results in the figure indicate that the combustion of hydrogen in the base region caused the base force to decrease and therefore the base drag to increase. This is unexpected since combustion should cause an increase in temperature and any increase in temperature would give rise to a decrease in base drag. Possibly the amount of hydrogen injected is too small and since it is located near the edge of the projectile the combusted gas mixes rapidly and is in effect quenched by the outer cooler stream.

The effects of combustion in the base region is shown in Figure 22 for the center injection case. Again the amount of hydrogen that was injected is the same as in the previous cases The results in the figure indicate that for the central injection, the combustion of a small amount of hydrogen in the base region initially causes the base force to increase (I=.01) and therefore the base drag to decrease. As the amount of mass flow increases, however, this trend reverses itself and at mass injection ratios greater than .025 the base force is smaller than for the no injection case.

In obtaining these results the base force did not attain a steady state value. The base force time history for these four injection cases are shown in Figure 23. All of the cases demonstrated an almost constant value of base force at early values of time. At later values of time this force increased. It is not known if this behaviour is due to improper implemenation of the injectant boundary conditions, downstream boundary conditions or reflections from the downstream boundaries that traveled back to the base region. Each of these effects can be investigated by moving the downstream boundary or using different boundary conditions such as characteristics rather than extrapolated boundary conditions.

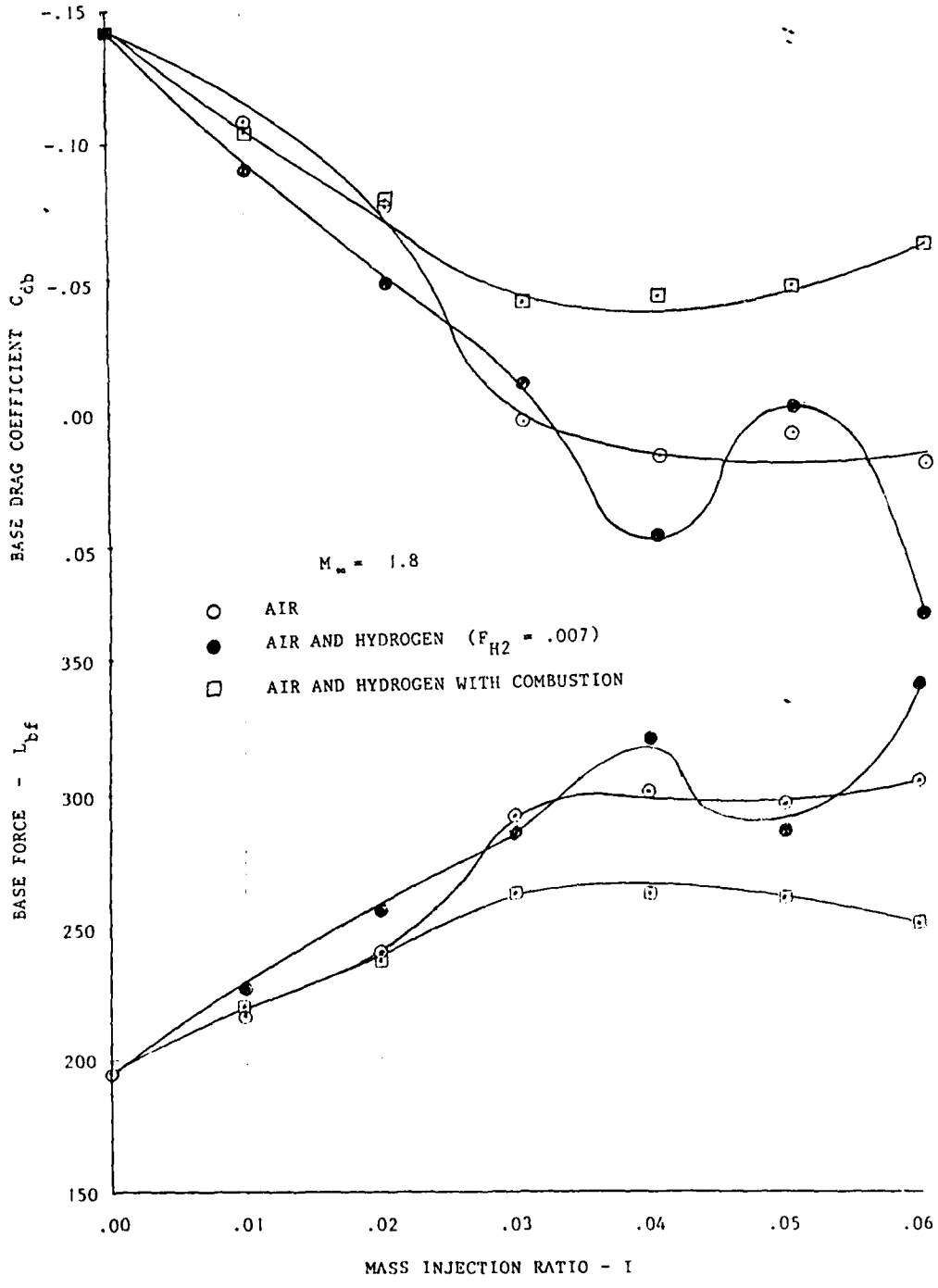

EDGE INJECTION - AIR AND HYDROGEN WITH COMBUSTION

FIGURE 21

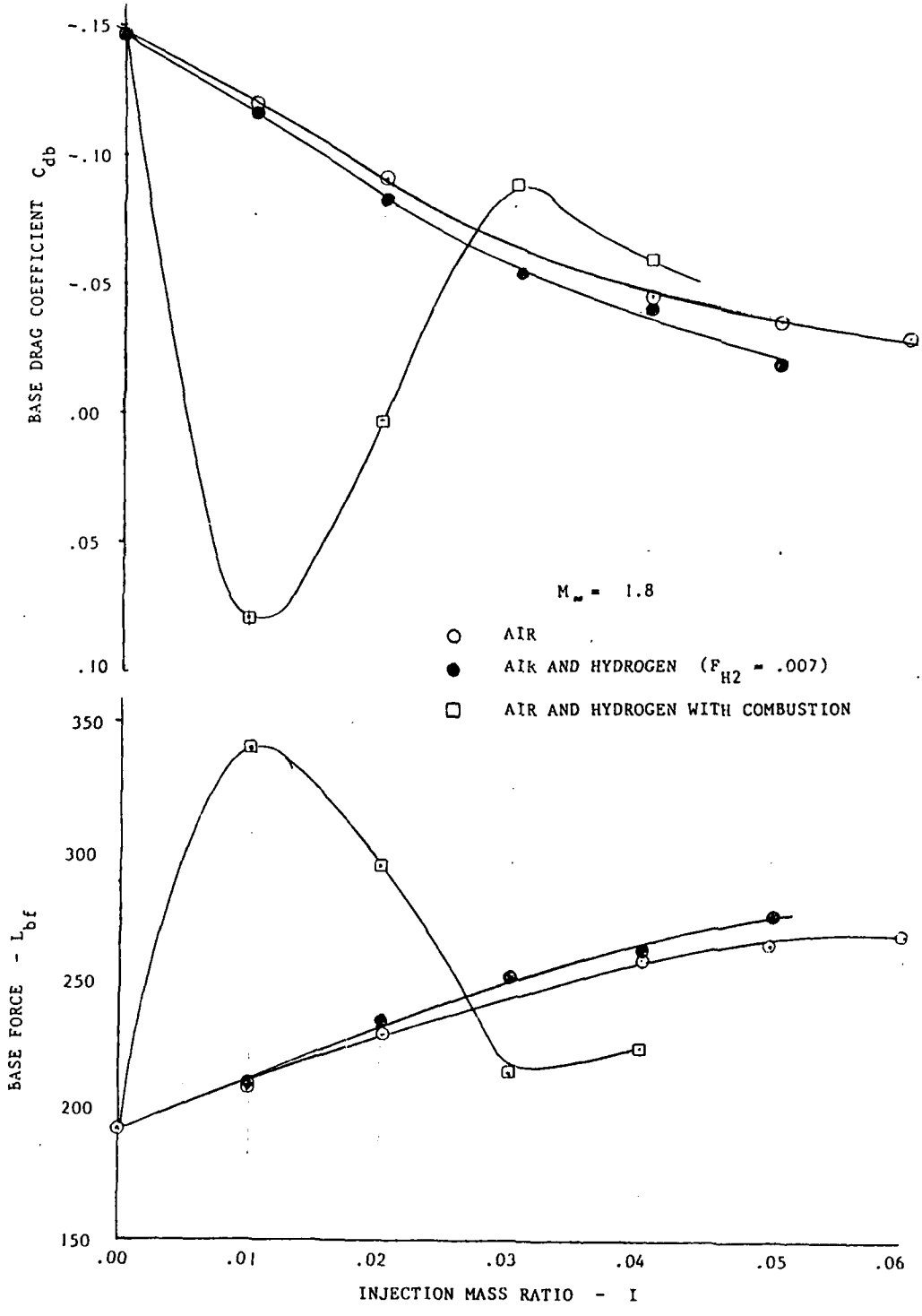

CENTER INJECTION - AIR AND HYDROGEN WITH COMBUSTION

FIGURE 22

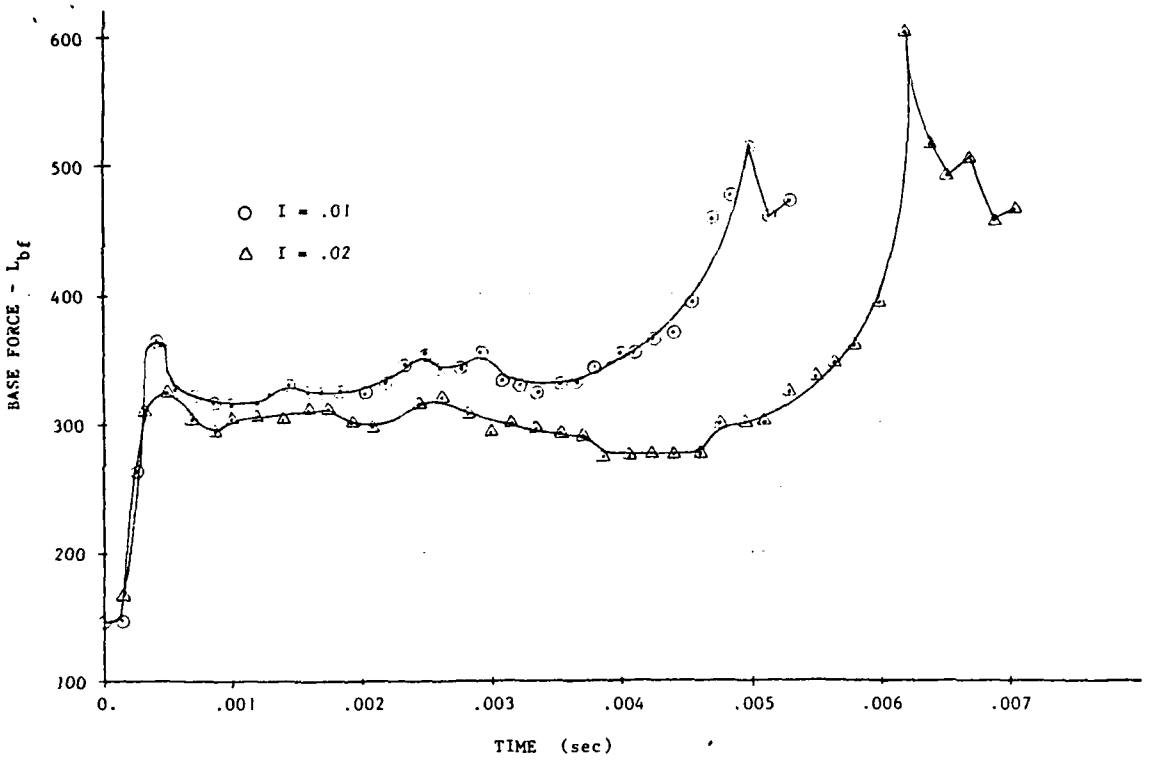

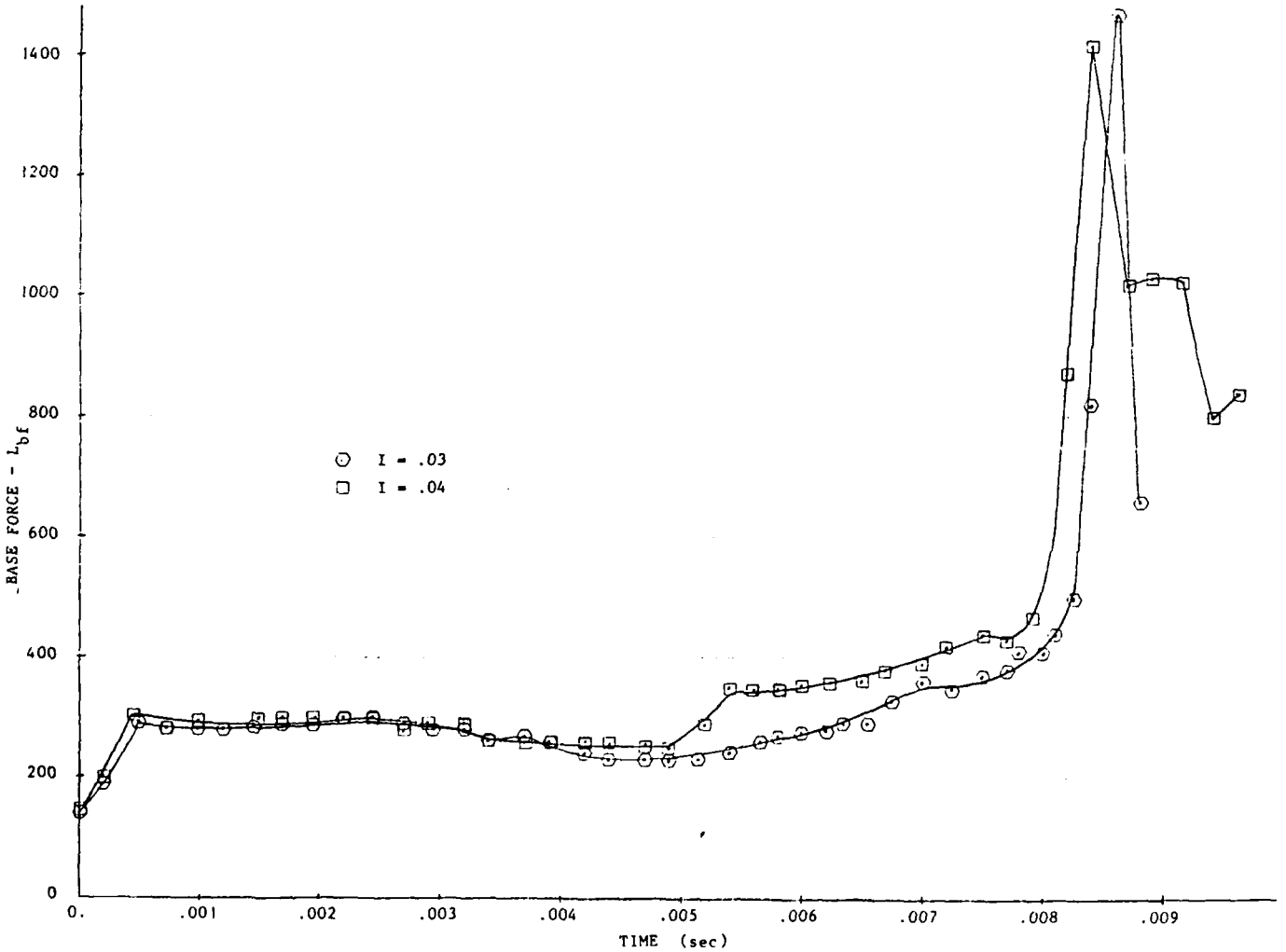

BASE FORCE TIME HISTORY

FIGURE 23

A problem area that surfaced during the performance of the theoretical calculations was the base force in some cases did not readily converge to a constant value. The degree of oscillation is depicted in Figure 24 for a case with no injection and in Figure 25 for a case where the injectant mass flow ratio was .01 and the free stream Mach number was 2.2. This oscillation is believed to be due to applying a constant value of pressure over the injection plane where in reality the pressure and velocity vary over the injection plane. This effect or variation would be more dominant for large bodies with sparser grids than for smaller diameter bodies with more tightly clustered grids. Comparison to the no injection case shows that the base force converges very rapidly to a constant value after only about 4000 iterations. Except for the peak that occurs at about 5000 iterations the value is extremely steady. This indicates that further work must be done to either smooth the flow in the base injection region or to allow for a variable injectant conditions at the injectant plane.

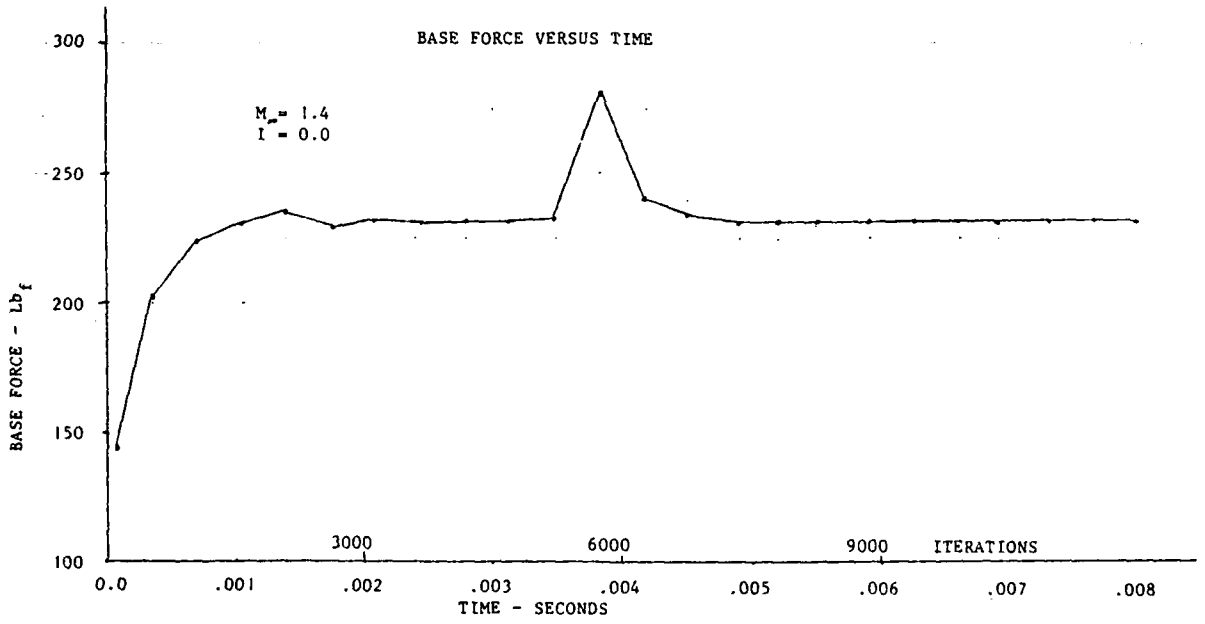

BASE FORCE TIME HISTORY
FIGURE 24

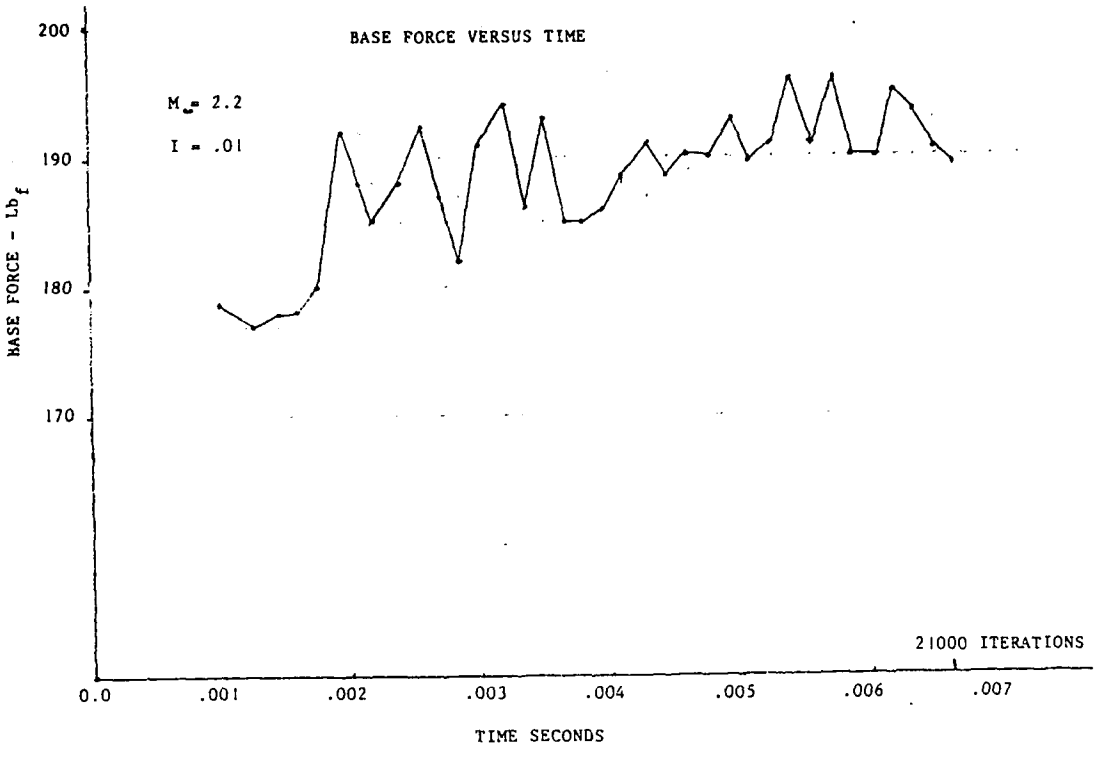

BASE FORCE TIME HISTORY WITH INJECTION

FIGURE 25

Conclusions

The results obtained indicate that subsonic base injection can be beneficial in reducing base drag. The use of edge injection gives higher values of base drag reduction (by approximately 20%) than center injection. Use of higher temperature injectant gas also gives larger values of base drag reduction. It appears that small injection amounts of burning gas in the base region is more beneficial than large amounts, which might blow off the base bubble.

Details of the optimum injection scheme, however, still remain to be determined. In particular, effects of flow channels located in the base region that direct the flow either radially inward or outward may increase or possibly decrease the base pressure and therefore alter the range of the artillery shell. Potential flow channel concept are illustrated in Figure 26. The objective of these concepts are to direct injectant gas so that it interacts with ambient air that is trying to turn the corner or to use bleed paths to generate small jets which interact with the gaseous injectant.

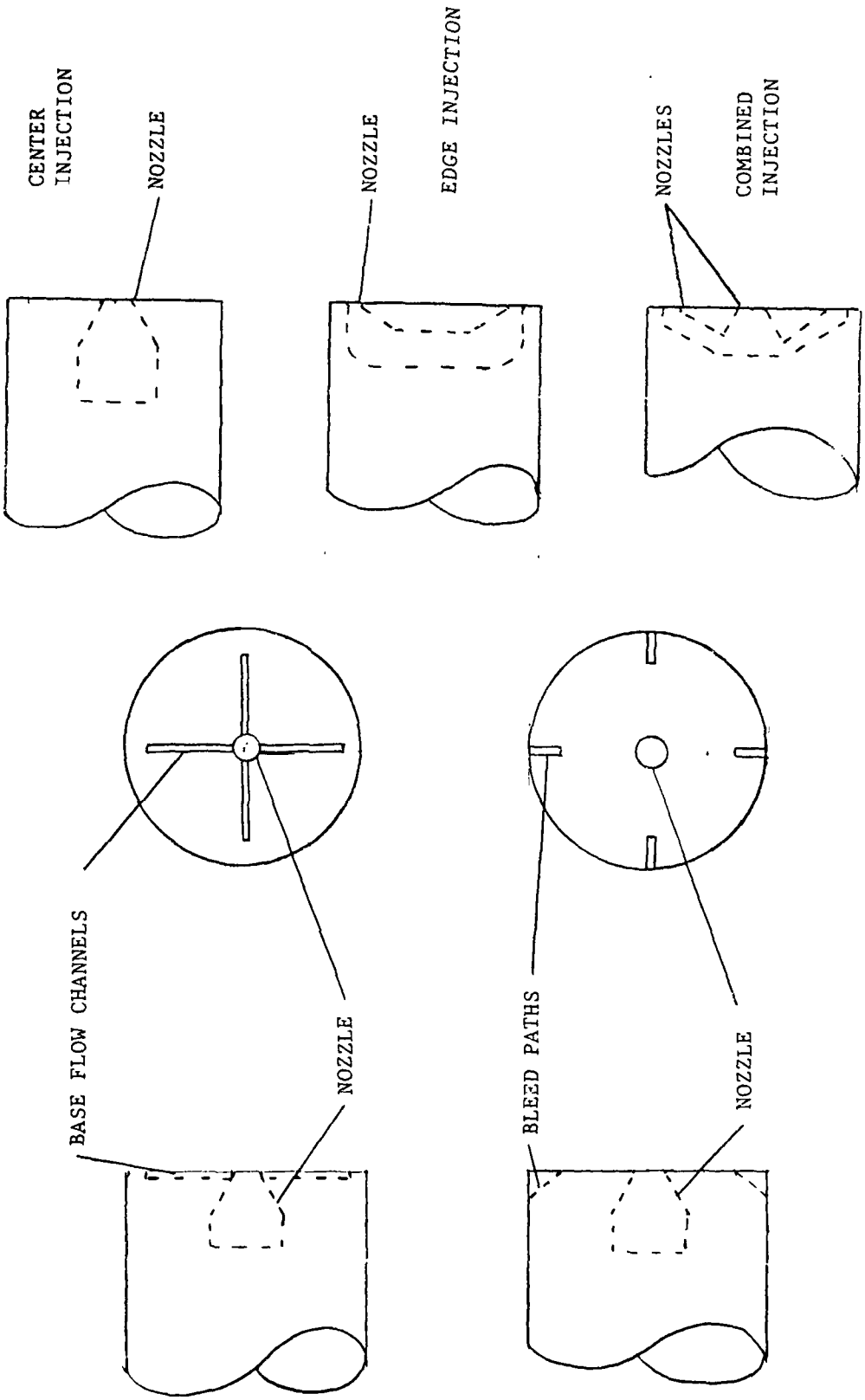

POTENTIAL BASE BLEED CONFIGURATIONS

FIGURE 26

REFERENCES

1. Nakahashi, K. and Diewert, G.S. "A Practical Adaptive Grid Method for Complex Fluid-Flow Problems" NASA TM-85890, June 1984

2. Chapman, D.R., "An Analysis of Base Pressure at Supersonic Velocities and Comparison with Experiment" NACA 1051 1951

3. Sahu, J "Supersonic Flow Over Cylindrical Afterbodies with Base Bleed" AIAA 86-0487, January 1986

4. Cavalleri, R.J. "Assessment of a Time-Dependent Computational Technique for Chemical Laser Type Diffuser Flowfield Calculations" AIAA Paper II-6 Presented at the AIAA Conference on Fluid Dynamics of High Power Lasers October, 1978

5. Drummond, J.P. and Weidner, E.H., "Numerical Study of a Scramjet Engine Flowfield", AIAA Journal 1982, Vol. 20 No. 9 pp. 1182-1187

6. Drummond, J.P. "Numerical Study of a Ramjet Dump Combustor Flowfield", AIAA-83-0421, 1983

7. MacCormack. R.W. "The Effect of Viscosity on Hypervelocity Impact Cratering", AIAA Paper 69-354, 1969

8. Schetz, J.A. "Analysis of The Mixing and Combustion of Gaseous and Particle Laden Jets in an Air Stream", AIAA Paper 69-33, Presented at the AIAA 7th Aerospace Sciences Meeting January 1969

LIST OF SYMBOLS

A	Area
C_{db}	base drag coefficient $2(F_b-F_\infty)/(\rho u^2)_\infty$
F_b	base drag force
F_∞	reference base force ($A_b p_\infty$)
I	mass injection ratio
m	mass flow rate
M	Mach number
p	pressure
R	gas constant
R_θ	circumferential viscous terms
T	temperature
u	x direction velocity
v	y direction velocity
w	circumferential velocity
x	axial distance
y	vertical distance
γ	ratio of specific heats
θ	circumferential co-ordinate
μ	viscosity
ρ	density
Ω	angular velocity

SUBSCRIPTS

b	base value
j	injectant value
o	injectant supply value
∞	free stream condition